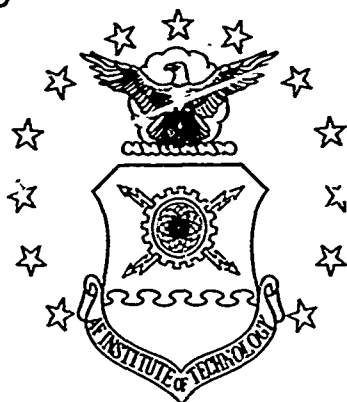
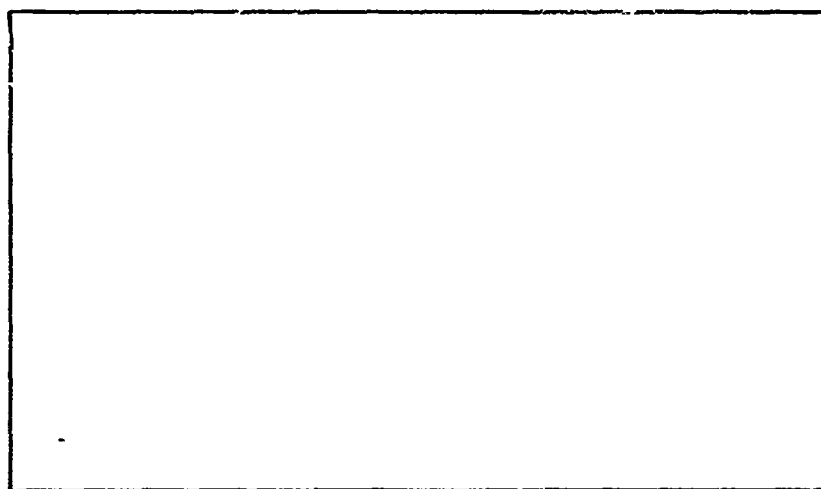


AD 746262

# AIR FORCE INSTITUTE OF TECHNOLOGY



AIR UNIVERSITY  
UNITED STATES AIR FORCE



## SCHOOL OF ENGINEERING

Reproduced by  
NATIONAL TECHNICAL  
INFORMATION SERVICE  
U.S. Department of Commerce  
Springfield VA 22151

WRIGHT-PATTERSON AIR FORCE BASE, OHIO

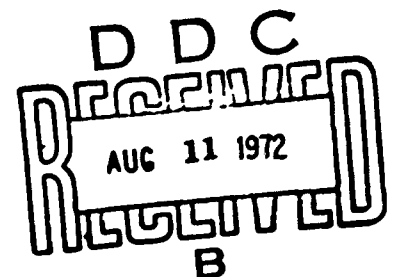
DDC  
RECEIVED  
AUG 11 1972  
76

AN INVESTIGATION INTO THE CAUSES  
FOR THE SHORT LIFETIMES OF GEIGER-  
MULLER TUBES USED IN AIRCRAFT OIL  
GAUGING SYSTEMS

THESIS

GEP/PH/72-14

Dale E. Morin  
Captain USAF



Approved for public release, distribution unlimited

DISTRIBUTION STATEMENT A

Approved for public release;  
Distribution Unlimited

UNCLASSIFIED

Security Classification

## DOCUMENT CONTROL DATA - R &amp; D

(Security classification of title, body of abstract and indexing annotation must be entered when the overall report is classified)

1. ORIGINATING ACTIVITY (Corporate author) Air Force Institute of Technology (AFIT-EN) Wright-Patterson AFB, Ohio 45433		20. REPORT SECURITY CLASSIFICATION Unclassified
3. REPORT TITLE An Investigation Into The Causes For The Short Lifetimes of Geiger-Müller Tubes Used in Aircraft Oil Gauging Systems		25. GROUP
4. DESCRIPTIVE NOTES (Type of report and inclusive dates) AFIT Thesis		
5. AUTHOR(S) (First name, middle initial, last name) Dale E. Morin Captain USAF		
6. REPORT DATE June 1972	7a. TOTAL NO. OF PAGES 53	7b. NO. OF REFS 33
8a. CONTRACT OR GRANT NO.	9a. ORIGINATOR'S REPORT NUMBER(S) GEP/PH/72-14	
b. PROJECT NO. 337A	9b. OTHER REPORT NO(S) (Any other numbers that may be assigned this report)	
c.		
d.		
10. DISTRIBUTION STATEMENT Approved for public release, distribution unlimited.		
Approved for public release; LAW AFR 190-17 Keith A. Williams, 1st Lt., USAF Acting Director of Information		17. SPONSORING MILITARY ACTIVITY
13. ABSTRACT The causes of failure of the G-M detectors used in the nucleonic oil gauging system of USAF aircraft are presented. Experimental tests performed on several tubes, in simulated aircraft environments, proved that the detectors fail because of a depletion of the halogen quench gas. A variety of surface analyses established that the halogen gas reacted with both the cathode and anode surfaces; On the cathode the halogen (bromine) attack was always co-located with lead deposits and the only known source of lead inside the counter is from the glass solder used as the tube sealant. The anode showed two types of bromine attack: A fairly uniform attack of the entire surface and a highly localized attack on abraded regions. These abrasions were evident on every detector that failed in the simulated aircraft environment. Recommendations are made to increase the G-M tube longevity. Implementing these recommendations require only minor modifications to the basic system.		

1a

DD FORM 1 NOV 65 1473

UNCLASSIFIED

Security Classification

UNCLASSIFIED

**Security Classification**

84

### KEY WORDS

LINK 2

**LINK E**

## LIN C

**RULE**

NT

	NAME	ROLE
1	JOHN J. ...	...
2	JAMES E. ...	...
3	JOHN F. ...	...
4	JOHN G. ...	...
5	JOHN H. ...	...
6	JOHN I. ...	...
7	JOHN K. ...	...
8	JOHN L. ...	...
9	JOHN M. ...	...
10	JOHN N. ...	...
11	JOHN O. ...	...
12	JOHN P. ...	...
13	JOHN Q. ...	...
14	JOHN R. ...	...
15	JOHN S. ...	...
16	JOHN T. ...	...
17	JOHN U. ...	...
18	JOHN V. ...	...
19	JOHN W. ...	...
20	JOHN X. ...	...
21	JOHN Y. ...	...
22	JOHN Z. ...	...
23	JOHN A. ...	...
24	JOHN B. ...	...
25	JOHN C. ...	...
26	JOHN D. ...	...
27	JOHN E. ...	...
28	JOHN F. ...	...
29	JOHN G. ...	...
30	JOHN H. ...	...
31	JOHN I. ...	...
32	JOHN K. ...	...
33	JOHN L. ...	...
34	JOHN M. ...	...
35	JOHN N. ...	...
36	JOHN O. ...	...
37	JOHN P. ...	...
38	JOHN Q. ...	...
39	JOHN R. ...	...
40	JOHN S. ...	...
41	JOHN T. ...	...
42	JOHN U. ...	...
43	JOHN V. ...	...
44	JOHN W. ...	...
45	JOHN X. ...	...
46	JOHN Y. ...	...
47	JOHN Z. ...	...
48	JOHN A. ...	...
49	JOHN B. ...	...
50	JOHN C. ...	...
51	JOHN D. ...	...
52	JOHN E. ...	...
53	JOHN F. ...	...
54	JOHN G. ...	...
55	JOHN H. ...	...
56	JOHN I. ...	...
57	JOHN K. ...	...
58	JOHN L. ...	...
59	JOHN M. ...	...
60	JOHN N. ...	...
61	JOHN O. ...	...
62	JOHN P. ...	...
63	JOHN Q. ...	...
64	JOHN R. ...	...
65	JOHN S. ...	...
66	JOHN T. ...	...
67	JOHN U. ...	...
68	JOHN V. ...	...
69	JOHN W. ...	...
70	JOHN X. ...	...
71	JOHN Y. ...	...
72	JOHN Z. ...	...
73	JOHN A. ...	...
74	JOHN B. ...	...
75	JOHN C. ...	...
76	JOHN D. ...	...
77	JOHN E. ...	...
78	JOHN F. ...	...
79	JOHN G. ...	...
80	JOHN H. ...	...
81	JOHN I. ...	...
82	JOHN K. ...	...
83	JOHN L. ...	...
84	JOHN M. ...	...
85	JOHN N. ...	...
86	JOHN O. ...	...
87	JOHN P. ...	...
88	JOHN Q. ...	...
89	JOHN R. ...	...
90	JOHN S. ...	...
91	JOHN T. ...	...
92	JOHN U. ...	...
93	JOHN V. ...	...
94	JOHN W. ...	...
95	JOHN X. ...	...
96	JOHN Y. ...	...
97	JOHN Z. ...	...
98	JOHN A. ...	...
99	JOHN B. ...	...
100	JOHN C. ...	...

NT

NAME	ROLE
1. [Name]	[Role]
2. [Name]	[Role]
3. [Name]	[Role]
4. [Name]	[Role]
5. [Name]	[Role]
6. [Name]	[Role]
7. [Name]	[Role]
8. [Name]	[Role]
9. [Name]	[Role]
10. [Name]	[Role]
11. [Name]	[Role]
12. [Name]	[Role]
13. [Name]	[Role]
14. [Name]	[Role]
15. [Name]	[Role]
16. [Name]	[Role]
17. [Name]	[Role]
18. [Name]	[Role]
19. [Name]	[Role]
20. [Name]	[Role]
21. [Name]	[Role]
22. [Name]	[Role]
23. [Name]	[Role]
24. [Name]	[Role]
25. [Name]	[Role]
26. [Name]	[Role]
27. [Name]	[Role]
28. [Name]	[Role]
29. [Name]	[Role]
30. [Name]	[Role]
31. [Name]	[Role]
32. [Name]	[Role]
33. [Name]	[Role]
34. [Name]	[Role]
35. [Name]	[Role]
36. [Name]	[Role]
37. [Name]	[Role]
38. [Name]	[Role]
39. [Name]	[Role]
40. [Name]	[Role]
41. [Name]	[Role]
42. [Name]	[Role]
43. [Name]	[Role]
44. [Name]	[Role]
45. [Name]	[Role]
46. [Name]	[Role]
47. [Name]	[Role]
48. [Name]	[Role]
49. [Name]	[Role]
50. [Name]	[Role]
51. [Name]	[Role]
52. [Name]	[Role]
53. [Name]	[Role]
54. [Name]	[Role]
55. [Name]	[Role]
56. [Name]	[Role]
57. [Name]	[Role]
58. [Name]	[Role]
59. [Name]	[Role]
60. [Name]	[Role]
61. [Name]	[Role]
62. [Name]	[Role]
63. [Name]	[Role]
64. [Name]	[Role]
65. [Name]	[Role]
66. [Name]	[Role]
67. [Name]	[Role]
68. [Name]	[Role]
69. [Name]	[Role]
70. [Name]	[Role]
71. [Name]	[Role]
72. [Name]	[Role]
73. [Name]	[Role]
74. [Name]	[Role]
75. [Name]	[Role]
76. [Name]	[Role]
77. [Name]	[Role]
78. [Name]	[Role]
79. [Name]	[Role]
80. [Name]	[Role]
81. [Name]	[Role]
82. [Name]	[Role]
83. [Name]	[Role]
84. [Name]	[Role]
85. [Name]	[Role]
86. [Name]	[Role]
87. [Name]	[Role]
88. [Name]	[Role]
89. [Name]	[Role]
90. [Name]	[Role]
91. [Name]	[Role]
92. [Name]	[Role]
93. [Name]	[Role]
94. [Name]	[Role]
95. [Name]	[Role]
96. [Name]	[Role]
97. [Name]	[Role]
98. [Name]	[Role]
99. [Name]	[Role]
100. [Name]	[Role]

W T

## Geiger-Müller Tubes Used on Aircraft

## Geiger-Müller Tubes Used in High Temperatures and Vibration

## Geiger-Müller Counter Efficiency

## Halogen Attack of Geiger-Müller Tube Surfaces

1h

UNCLASSIFIED

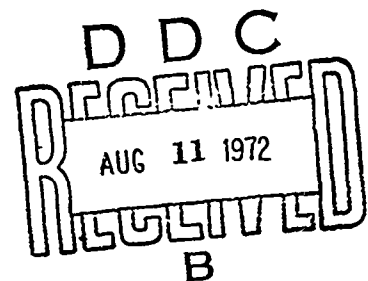
Security Classification

AN INVESTIGATION INTO THE CAUSES  
FOR THE SHORT LIFETIMES OF GEIGER-  
MULLER TUBES USED IN AIRCRAFT OIL  
GAUGING SYSTEMS

THESIS

GEP/PH/72-14

Dale E Morin  
Captain USAF



Approved for public release, distribution unlimited

DISTRIBUTION STATEMENT A

Approved for public release;  
Distribution Unlimited

AN INVESTIGATION INTO THE CAUSES  
FOR THE SHORT LIFETIMES OF GEIGER-  
MULLER TUBES USED IN AIRCRAFT OIL  
GAUGING SYSTEMS

THESIS

Presented to the Faculty of the School of Engineering  
of the Air Force Institute of Technology  
Air University  
in Partial Fulfillment of the  
Requirements for the Degree of  
Master of Science  
by

Dale E. Morin, B.S.  
Captain USAF  
Graduate Engineering Physics  
June 1972

Approved for public release, distribution unlimited.

ic

Preface

Any problem which inhibits the operational readiness of our Air Force, should be solved in the most rapid manner possible. This was my feeling when I was assigned the task of solving the "short-life" problem inherent in the Geiger-Muller tubes presently used on USAF aircraft. When I was introduced to the problem, it was extremely hard for me to realize how this small and "simple-looking" device could possibly have the impact on aircraft operational status that it does. As time went by and my investigations became more involved, I found that this "simple" device became extremely complicated when placed in the thermal and vibrational environment of the airplane. It was a short time later when I concluded that I was going to need help. My cries for help were heard by far more people than I thought possible. It is to these people that I owe a debt of gratitude far greater than I can ever pay. Fortunately, their reward is the same as mine--the satisfaction of having worked on an "Air Force" problem and having been a part of the overall solution to that problem. Although this is all they asked for, I feel that without them little progress could have been made, and so, I am now going to attempt to put into words all the gratitude that I have felt during these past months.

The first person I came in contact with (outside my own laboratory), was Maj. Larry Fehrenbacher of the Aerospace Research Laboratory (ARL). Through him, nearly every door of ARL was literally opened at one time or another. It was his motivation and interest that made this problem mean more to me than just a "block to fill" and a "grade to record". The time, that he took away from his own research and study, was given willingly in the interest of solving an "operational problem". Through Major Fehrenbacher, I met Dr. Tiernan, Dr. Hughes and Mr. Michael Taylor of ARL's Chemistry Branch. These three men contributed significantly to this study. As in any investigation, problems arise and "dead-ends" are incurred. These people would not take "no" for an answer, and always found a new method of approach. The results they derived from spark source mass spectrometry were priceless.

Major Fehrenbacher also introduced me to Dr. W. Haas of the Surface Analysis Branch of ARL. His study of detector surfaces via Auger spectrometry, also gave a great insight into the attack that took place on these surfaces.

I am also indebted to Dr. W. Baun and Mr. James Solomon of the Air Force Materials Laboratory. Their analyses of G-M tube surfaces (by the scanning electron microprobe) provided many pictures of the corrosion that caused the detectors to fail.

In the Flight Dynamics Laboratory, there is one special person that gave me and my problems many hours of his off-duty time. This time was given at the expense of himself and his family, and so, to Capt. Denny Rossbach and his wife, I say "thank you".

There are two extremely important people, whom I feel, never really comprehended how much I appreciated their assistance: My thesis advisor Dr. George John and my laboratory advisor Capt. Robert Couch. Without their suggestions, questions, and answers this study would have been doomed to failure. In that this thesis was a success, directly reflects their dedication and sincerity. To Dr. John and Capt. Couch I extend my sincere gratitude.

There are many others to whom I would like to thank, but space prohibits it. So in short, I thank Mr. Brennan Gisclard, Mr. James Clark, Lt. Larry Tessler, the Harshaw Chemical Company and all those people who added to this study.

The last and greatest debt of gratitude is owed to my wife and family. Without their love, confidence, and patience, I could never have accomplished the task of gaining this degree.

This work was performed under the charge number 337A at the Air Force Flight Dynamics Laboratory, Control Systems Development Branch (FGL), Wright-Patterson AFB, Ohio.

Dayton, Ohio

Dale E. Morin

March 1972



## Contents

	Page
Preface .....	ii
List of Figures .....	vi
List of Tables .....	vi
Abstract .....	vii
I. Introduction.....	1
Problem .....	1
Background .....	1
Goals and Approach .....	1
II. Theoretical Considerations .....	3
Summary of Halogen-Quenched G-M Counter Operations .....	3
Description of Aircraft G-M Tubes .....	3
The Formation and Spread of the Discharge .....	3
The Initial Ionizing Process .....	3
The Spread of the Discharge .....	5
Quenching the Discharge .....	5
Known Aging Characteristics .....	7
The Effect of Aging on $V_s$ .....	7
The Effect of Aging on the Plateau .....	8
The Occurrence of Oscillations in Aged Tubes .....	8
Recommendations for Extending the Lifetime of G-M Tubes .....	9
III. Experimental Equipment .....	10
The Geiger-Muller Tubes .....	10
The Electronic Circuitry .....	11
The High Voltage Sources .....	11
The Pulse Detecting and Recording Equipment .....	11
The Radiation Sources .....	12
IV. Experimental Tests, Procedures and Results .....	13
Introduction .....	13
Analysis of a New G-M Tube .....	14
The Spark Source Spectrometer Analysis .....	14
The Auger Spectrometer Analysis .....	14
The Scanning Electron Microprobe Analysis .....	14
The Wet Chemical Gas Analysis .....	14
The Mass Spectrometer Gas Analysis .....	14
Lifetime Testing of G-M Tubes in 200°C Temperature .....	14
Procedures .....	15
Results .....	15
The Aging Characteristics .....	15
The Wet Chemical Gas Analysis .....	16
The Spark Source Spectrometer Analysis .....	16

Lifetime Testing of G-M Tubes in a Simulated Aircraft Environment .....	16
Procedures .....	17
Results .....	18
The Aging Characteristics .....	18
The Spark Source Spectrometer Analysis .....	21
Analysis by Auger Spectrometry .....	21
The Scanning Electron Microprobe Analysis .....	21
The Wet Chemical Gas Analysis .....	23
The Mass Spectrometer Gas Analysis .....	23
Summary .....	23
The Efficiency Experiment .....	24
Introduction .....	24
Procedures .....	25
Efficiency vs Counter Dimensions .....	25
Efficiency vs Cathode Materials .....	25
Results .....	25
Summary .....	26
The Vibration Experiment .....	26
Introduction .....	26
Procedures .....	27
Results .....	27
Summary .....	27
V. Conclusions and Recommendations .....	29
Conclusions .....	29
From the Environmental Experiments .....	29
From the Supplementary Experiments .....	29
Recommendations .....	30
Immediate Modifications .....	30
Interim Changes .....	31
Recommendations for Further Study .....	31
Bibliography .....	35
Appendix A      A Detailed G-M Tube Theory .....	37
Appendix B      The Composition, Halogen-Resistance, and Vibrational Characteristics of Various Materials .....	47
Appendix C      Gas and Surface Analysis Methods .....	50
Appendix D      Graphic Data of the Changes in $V_s$ During the Environmental Tests .....	52
VITA .....	55

List of Figures

Figure		Page
1	A Harshaw Geiger-Muller Tube	10
2	The Fundamental Sensing Circuit Used in Experimental Testing	11
3	Typical G-M Tube Plateau	12
4	Graph of simulated Aircraft Vibrations	17
5	Geiger Pulse - - No Pulse Height Control	18
6	Geiger Pulse - - Manual Pulse Height Control With $V_B < V_C$	18
7	Geiger Pulse - - Automatic Pulse Height Control	18
8	"Damped" Oscillation	20
9	Cross-section Scan of Cathode for Pt	22
10	Cross-section Scan of Cathode for Ni	22
11	Cross-section Scan of Cathode for Fe	22
12	Cross-section Scan of Cathode for Crq	22
13	Lead Spot on Cathode	22
14	X-ray Scan of the Lead Spot (in Fig. 13) For Bromine	22
15	Bromine Attack on the Anode	22
16	Efficiency vs Cathode Diameter	25
17	Efficiency vs Cathode Length	25
18	Oscilloscope Displayed Geiger Pulse	42
19	Dead Time and Recovery Time	42
20	Nomograph for Determining $V_n$	44

List of Tables

Table Number	Title	Page
I	Results of the Analysis on a New Tube .....	14
II	Results From the Thermal Environment Test .....	15
III	Results From the Combined Environment Test .....	19
IV	Counter Materials Composition and Vibrational Characteristics .....	50

Abstract

The causes of failure of the G-M detectors used in the nucleonic oil gauging system of USAF aircraft are presented. Experimental tests performed on several tubes, in simulated aircraft environments, proved that the detectors fail because of a depletion of the halogen quench gas. A variety of surface analyses established that the halogen gas reacted with both the cathode and anode surfaces. On the cathode the halogen (bromine) attack was always co-located with lead deposits and the only known source of lead inside the counter is from the glass solder used as the tube sealant.

The anode showed two types of bromine attack: A fairly uniform attack of the entire surface and a highly localized attack on abraded regions. These abrasions were evident on every detector that failed in the simulated aircraft environment.

Recommendations are made to increase the G-M tube longevity. Implementing these recommendations require only minor modifications to the basic system.

## I. Introduction

### Problem

The operational readiness of approximately 1500 aircraft, which employ the nucleonic oil gauging system, has been impaired by the failure of the Geiger-Muller (G-M) detectors used as sensors in this system. This thesis reports the causes of failure and the methods for increasing the longevity of G-M detectors in the high-temperature and vibrational environment of the jet engine.

### Background

Until recently, the method most used to ascertain the presence of oil in the engine (during flight) was a pressure-sensing system. Unfortunately, the pressure in the oil lines remains almost constant until the oil reservoir is empty and under optimum conditions the engine will continue to operate for only another 15 minutes. Thus, a means of ascertaining "real" time measurements of the oil quantity is extremely advantageous. The nucleonic oil gauging system is capable of giving this information and has been credited with saving several airplanes. As an additional emphasis, the Tactical Air Command has made this system mandatory on all new single-engine aircraft.

### Goals and Approach

In light of the need for more rugged G-M tubes, this thesis has as its goals:

1. To determine how and why the aircraft G-M tubes fail so rapidly,
2. To determine how their useful lifetimes may be extended, and
3. To develop a truly rugged, long life G-M tube.

A review of G-M tube theory is presented as a first step in approaching this problem. This review stresses the aging characteristics, causes of failure, and methods of extending a counters lifetime and is used as a comparison and guide throughout the experimental section.

The second section reports the results gained from the two experimental areas: The environmental tests and the supplementary tests. The environmental tests were conducted under highly controlled conditions, designed to reproduce the temperatures and vibrations of the jet engine. The results of these tests (performed on new tubes) are compared with aging and failure characteristics gained from literature searches. The data gathered from elaborate surface analyses performed on numerous detectors is reported and shows exactly how and why these detectors failed.

The results of the supplementary tests are used to illustrate how the materials and design of aircraft G-M tubes can be adjusted so that extensions to operational lifetimes are achieved.

GEP/PH/72-14

In the last section (Conclusions and Recommendations) methods are suggested by which the aircraft detectors can be modified to increase their longevity and yield a truly rugged G-M tube.

## II. Theoretical Considerations

The basic theory of halogen-quenched G-M counters must be understood, so that comparisons can be made and conclusions drawn from the results of the experimental tests. The following is a summary of that theory which is presented in greater detail in Appendix A.

### Summary of Halogen-Quenched G-M Counter Operations

The theory of G-M tube operations has been studied extensively by Rose, Korff, Present, Liebson, Curran, Craggs, Friedman, Loeb and a number of others who have contributed to the development of the fundamental principles. In order to summarize their works clearly and as concise as possible, the theory is presented in five main parts. The parts are presented in the order in which they are listed:

1. The description of aircraft G-M tubes,
2. The formation and spread of the discharge,
3. The process of quenching the discharge,
4. The aging characteristics of G-M tubes, and
5. The recommendations for increasing the longevity of G-M tubes.

The Description of Aircraft G-M Tubes. Halogen-quenched G-M tubes are presently used on USAF aircraft, and consist of two concentric cylinders. The inner cylinder, or anode, is a taut wire, which is maintained at a positive potential and insulated from the outer cylinder (or cathode). The space between these two cylinders is filled, to a pressure of approximately one-half atmosphere, with a gas mixture. This mixture is a combination of approximately 98.4 percent neon, 0.1 percent argon and 1.5 percent halogen (bromine or chlorine), where the neon gas acts as the "carrier" of the discharge. The actual tubes used on aircraft, are discussed in further detail in the Experimental Equipment section and also in Ref 22:i-12.

The Formation and Spread of the Discharge. This section explicates the essentials of radiation detection: The initial ionization process and the spread of the discharge.

1. The Initial Ionization Process. This process can be initiated only if three conditions are met:

1. The potential on the anode must be greater than or equal to the starting voltage ( $V_s$ ) of the detector,
2. The detector must be in a radiation field, and
3. An electron must penetrate into the sensitive volume between the cathode and anode.

The first condition is necessary so that the field between the cylinders is great enough to support a

discharge. The second and third conditions are closely related, since it is the radiation field which gives rise to the electrons that penetrate the sensitive volume. To review some of the characteristics of this field will aid in understanding the overall ionization processes. A radiation field is composed of  $\alpha$ ,  $\beta$ ,  $\gamma$ , and x-radiation with energies characteristic of the emitting source. As stated in the Introduction, the source used on the aircraft is  $\text{Kr}^{85}$ , which emits a  $\beta \sim 0.67$  MeV (maximum) and a  $\gamma = 0.52$  MeV. The emitted photons ( $\gamma$  particles) generate the electrons that penetrate the sensitive volume and eventually cause the discharge to occur. However, prior to discussing the discharge formation, more consideration should be given to the generation of these electrons.

There are three mechanisms by which electrons can be produced:

1. Pair production,
2. Photoelectric effect in the gas or cathode walls, and
3. Compton effect in the gas or cathode walls.

Pair production requires an energy greater than 1.02 MeV to occur with any significant probability. Since  $\text{Kr}^{85}$  emits no photons at or above this energy, then pair production is of no interest.

Photoelectric and Compton effects also depend upon the energy of the photon, but both are possible at energies below 1.02 MeV, and definitely occur when  $\text{Kr}^{85}$  is used. These effects are also dependent upon the density and atomic number of the cathode material. From considerations of density and cross-sections of the gas and cathode walls, it can be assumed that both photoelectric and Compton events will occur most probably in the cathode walls (as a matter of fact, both of these processes do occur and are of nearly equal importance). Therefore, these processes in the cathode walls constitute the primary sources of energetic electrons, that initiate discharges in the G-M tube.

Once an energetic electron has penetrated the sensitive volume, it drifts toward the anode under the influence of the electric field (E). This field is characteristic of one formed between two concentric cylinders and varies according to the following equation:

$$E = \frac{V}{r \ln \frac{r_b}{r_a}} \quad (1)$$

where V is the potential applied to the anode wire and  $r_a$  and  $r_b$  are the radii of the anode and cathode respectively such that  $r_a < r < r_b$ . As the electron traverses the sensitive volume of the detector, it collides with neon atoms, producing ion pairs. The electrons from these ion pairs also drift toward the anode under the influence of the E-field and when they are near the center wire [approximately 5 wire radii (Ref 32:170)], they will have gained sufficient kinetic energy to produce additional ion pairs. These in turn, produce more ionization in a cascading process, which eventually results in a discharge that



completely encompasses the anode wire. The formation of the initial discharge in this manner is common to both G-M tubes and proportional counters. However, the spread of this discharge down the anode differentiates Giger-Muller tubes from proportional counters.

2. The Spread of the Discharge. The actual mechanism for the spread of a discharge, was unexplained for a long time, although photons were always considered to play an important role. The best current explanation is that the photons emitted from the energetic species of an avalanche, have wide varieties of energies and thus ionize other atoms or molecules in the gas. Through ionization, electrons are released which feed a new avalanche and thus the process continues. This ionizing process will now be discussed in greater detail to show the source of photons and what species can subsequently be ionized.

Neon is the most likely candidate, as the photon generating species, since it comprises over 98 percent of the mixture and argon combined with the halogen gas only constitutes 2 percent of the mixture. Therefore, the photons radiated by neon must now ionize some other molecule or atom in the mixture. It is not likely that a neon generated photon will have sufficient energy to ionize another neon atom, nor is it probable that argon, in its small percentage, could significantly add to this process and the same could be said of the halogen gas, since neither bromine or chlorine appreciably absorb photons (Ref 31:345). Thus, if the process is to continue, an additive absorption of energies (collisional and photon) must lead to ionization of neon atoms. Each successive avalanche moves the discharge slightly further down the wire, until the entire length has been traversed. The velocity of this spread has been measured by several observers to be approximately  $10^7$  cm/sec (Refs 15:179, 32:192). The end result of the discharge spread is a pulse whose height is independent of the initial ionizing event.

This section has shown how the discharge is formed, spreads the length of the anode, and yields a pulse that can be detected. The original discharge must now be quenched, to prevent the possibility of subsequent discharges (which would yield spurious counts).

Quenching the Discharge. The G-M counter is only accurate if it produces an output pulse rate proportional to incident radiation rate. Thus, each discharge originated by an ionizing event, must be terminated. This terminating process is known as quenching and is accomplished by:

1. The positive ion sheath,
2. The internal gases, and
3. The external circuitry.

As the discharge forms and traverses the counter length, the electrons are collected on the anode

leaving a positive-ion sheath surrounding the wire. This sheath reduces the E-field near the center wire, decreasing the probability of an avalanche forming, and in this way, acts as a quenching mechanism.

The positive ion sheath then drifts radially outward toward the cathode and when it has reached a critical distance [critical radius ( $r_c$ )] from the center wire, the field near the anode increases sufficiently that another avalanche and discharge can occur. The positive-ion sheath thus succeeds in delaying a second discharge from occurring, however, once it has moved past  $r_c$ , another discharge could form and thus give spurious counts. In order to prevent this, the energetic species created in the discharge, are neutralized by using quench gases. During the discharge, the metastable states of neon are readily excited and if allowed to exist, would eventually radiate enough energy to re-initiate the discharge. However, argon, bromine, and chlorine have ionization potentials below the neon metastable-state energy level. Thus, a collision between the metastable-state and any of the other gas atoms mentioned, results in a neon metastable de-excitation. When a neon metastable atom collides with an argon atom the argon is ionized in the process. The argon ions then drift in the E-field toward the cathode, but "charge exchange" with a halogen molecule before they reach the cathode.

The same basic neutralizing process is followed when a collision occurs between excited neon atoms and halogen molecules, except that the ionized halogen molecules will be neutralized by absorbing an electron from the cathode wall. Upon neutralization, the halogen molecule dissociates into two highly reactive atoms. These atoms eventually recombine to form a neutral halogen molecule, if chemical reactions with the internal surfaces do not occur first. This illustrates both the greatest advantage and disadvantage of using halogen gases. Since the dissociated halogen molecule will recombine to form the original quenching gas implies that the detector should last indefinitely. However, since these dissociated species are highly reactive, special precautions must be taken to insure that all the internal surfaces are totally halogen resistant. Although halogen gases definitely quench the discharge, the resulting plateaus (count-rate versus applied voltage) are generally short and steep, and a third quenching mechanism is needed to increase the effective voltage range of the G-M tube.

The entire quenching process can also be performed by the use of electrical circuits, but traditionally the recovery time (i.e., the time required for the positive-ion sheath to be neutralized) is very slow. External circuitry can be used in two ways to quench the discharge: Actively through quenching circuits, and passively by increasing the impedance of the sensing circuit. The active quenching process is not used on aircraft and thus will not be explained in this account. However, if further information is desired, reference is made to Price (Ref 25-118-123).

The passive quenching process is used in the nucleonic oil gauging system and its operation is explained next. As a preliminary investigation to this thesis, a simple experiment was performed

in which a counter was operated in a circuit with "zero" impedance. The result was that the counter began operating normally at  $V_s$  and the internal (space charge) mechanisms were sufficient to quench the discharge up to a certain voltage, called the critical voltage ( $V_c$ ). Once  $V_c$  was reached, two distinct pulse shapes were detected: A small pulse, which was the typical pulse noted below  $V_c$ , and a much larger pulse which was detected upon reaching  $V_c$ . The small pulses signified the discharges quenched by the internal mechanism and the large pulses were found to be quenched by a combination of circuit impedance and internal mechanisms.

In the low impedance circuit, the counter went into continuous discharge at  $V_c + \sim 10$  volts, but it was found that by increasing the circuit impedance, a greater voltage could be applied to the tubes before it would go into continuous discharge. This gave the counter a wider operating voltage span, or plateau. With this in mind, an additional resistance [load resistor ( $R_L$ )] was placed in series immediately behind the counter. In essence, the load resistance increases the circuit impedance and thus the operating range of the counter.

A second experiment was performed to determine the optimum circuit position for  $R_L$ . It was found that the advantageous effect of the load resistor was decreased as it was moved further from the G-M tube. This implies that, for best results, the load resistance should be as close as possible to the counter. Another result of this experiment indicated that the size of  $R_L$  is not as important as its presence or position, (i.e., a resistance of  $1.0M\Omega$  has the same basic effect as a  $5.0M\Omega$  resistor).

This completes the section on quenching the discharge. In summary, this account of the theory has: Described the tubes used on the aircraft, explained how the discharge process takes place and sprays, and finally, how the discharge is quenched so that a truly representative counting of the radiation field is attained. The next section in this account will deal with the known aging characteristics of G-M tubes.

#### Known Aging Characteristics

The importance of this section cannot be overstressed, for these aging characteristics will be used for guide lines throughout the remainder of this thesis. This section is divided into three parts, each dealing with one of the following characteristics:

1. The effect of aging on  $V_s$ ,
2. The effect of aging on the plateau, and
3. The occurrence of oscillations in aged tubes.

1. The Effect of Aging on  $V_s$  Starting voltage is defined herein as the potential that must be applied to the G-M counter in order to detect pulses with heights of  $\sim 20m$  volt. If this voltage were monitored during the aging of the tube, a decrease would be noted. This decrease is thought to be caused

by a depletion of the halogen gas through reactions with the internal surfaces of the counter. It has been assumed, by many authors, that these reactions are caused by the highly energetic dissociated halogen species and since they are formed close to the cathode, this surface should bear the brunt of the halogen attack. [Little significant data has been found to confirm this, or what (if any) attack is inflicted on the anode.] However, experiments performed by Liebson and Friedman and by Ward and Krumbein (Ref 19:304, 32:342), do prove that a decrease in  $V_s$  will accompany a reduction in the amount of halogen gas within the detector. Therefore, since the starting voltage can be monitored accurately and easily, this should be the first indication that any given tube is aging. Once the drop in  $V_s$  is significant, a study of the plateau should reveal considerable insight into the detectors' operational status.

2. The Effect of Aging on the Plateau. The second aging characteristic that should be noted is changes in the plateau. As was briefly mentioned before, the plateau is a plot of the count-rate of the detector versus the voltage that is applied to it. The length and slope of this plateau, depends upon a number of variables. Some of these are: the pressure in the chamber, the type of filling gas, the percentage of halogen gas, and the cathode material. However, for each set of initial conditions a corresponding plateau will exist and the changes in this curve are indicative of the detectors status.

In the last section, it was determined that the starting voltage should decrease with age. Assuming this is correct, then a corresponding shift in the starting point of the plateau should also occur. Again, from the first aging characteristic, it was noted that this reduction in  $V_s$  is due to a loss of halogen gas. If this is true, then as the halogen gas is depleted, the quenching ability of the detector is also reduced and the plateau should show a decrease in length. This reduction in quenching ability should also lead to an increase in the slope of the curve, since more spurious and multiple pulses can occur.

Thus, two different but related aging characteristics, can easily be followed and the status of the detector can likewise be monitored. There is one last characteristic that occurs in the aging process of a halogen G-M tube and this is discussed next.

3. The Occurrence of Oscillations in Aged Tubes. This last characteristic has been noted by many observers, but Liebson and Friedman were among the first (Ref 19:305). The most comprehensive and current explanation of this phenomena has been forwarded by Usacev and Seman (Ref 29:41-44). The oscillations noted in these references, generally occur in the vicinity of  $V_s$  and although there have been basically three different patterns noted, the frequency always lies in a range between 15Hz and 40 Hz. It must be realized that this phenomena occurs only when the amount of halogen gas is very small. Therefore, the oscillations are more indicative of failure rather than aging and they cannot really be used to monitor the status of a G-M tube.

In summary, there are two characteristics that can be continuously monitored to determine the operational status of the G-M tube (changes in  $V_g$  and changes in the plateau) and one phenomena that is more indicative of detector failure (oscillations). These three characteristics were used to evaluate the status of counters tested in this study.

Recommendations for Increasing the Longevity of G-M Tubes Before any recommendations can be made for extending the lifetime of G-M tubes, a review of how and why they fail is required.

From the aging characteristics it is noted that detectors age because the halogen gas is depleted. In theory, this depletion occurs when the dissociated halogen species react with the internal surfaces of the counter. Therefore, the only recommendation that theory forwards is to use halogen inert materials for the internal surfaces. The materials most referred to are: Stainless steel, tantalum and platinum. However, data gathered from corrosion handbooks (Ref 29:145, 321, 303) indicate that all these materials are attacked by halogens at temperatures above  $100^{\circ}\text{C}$  and this temperature is below those experienced on jet engines. Thus, it appears that part of this thesis must be devoted to finding new materials and methods for extending the lifetimes of G-M counters.

### III. Experimental Equipment

In this section the basic equipment used in the experimental portions of this thesis will be described. This description will not concern itself with the details of proprietary processes or the special equipment used in performing the analyses on failed G-M tubes. However, further information and references are given in Appendix C.

#### The Geiger-Muller Tubes

The halogen-quenched G-M tubes used throughout this study were basically the same as those employed in the A-7D aircraft and were manufactured by the Harshaw Chemical Company. These tubes have an overall and effective length of 5.5 inches and 3.8 inches respectively, and an outside diameter of 0.29 inches (see Fig.1).

The cathode is basically a 446 stainless steel cylinder, with a wall thickness of approximately 0.02 inches. The internal surfaces of the cathode undergo a series of proprietary processes which are designed to increase the detectors longevity and efficiency. One of the most important processes is an electroplated platinum layer on the cathode surface, which is approximately 15 microns thick and has a surface coverage of 8-15 mgms/cm<sup>2</sup> (Ref 22:4). Once the plating process is complete, then the surface undergoes oxidation and passivation steps to produce a halogen inert surface.

The anode is a 17-7 PH stainless steel wire whose diameter is about 25 mils. This wire is mounted in the detector under a tension in order to produce a resonant frequency between 800 Hz and 900 Hz. The wire, although not plated, undergoes the same oxidation and passivation processes as the cathode, and is insulated from the cathode through the use of forsterite insulators.

Once the G-M tube is assembled and sealed (using glass solder), the chamber is filled to a pressure of 350-400 torr with a gas mixture. This mixture is composed of 98.4 percent neon, 0.1 percent argon, and 1.5 percent bromine.

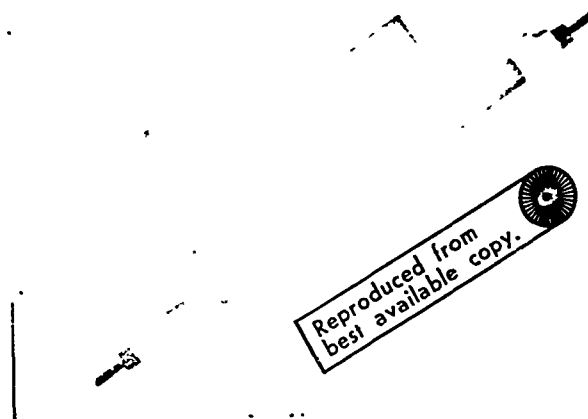


Fig. 1. A Harshaw Geiger-Muller Tube

### The Electronic Circuitry

The circuit employed in the experimental tests, to detect Geiger pulses, is shown in Fig. 2. The circuit is composed of; a high voltage source, a load resistor, ( $R_L$ ), a sensing resistor ( $R_S$ ), a capacitor (C), and a G-M tube. Although various high voltage sources were employed, the discussion of these will be postponed to the electronic equipment section. Both the load resistor (when used) and the sensing resistor were about  $5M\Omega$ .

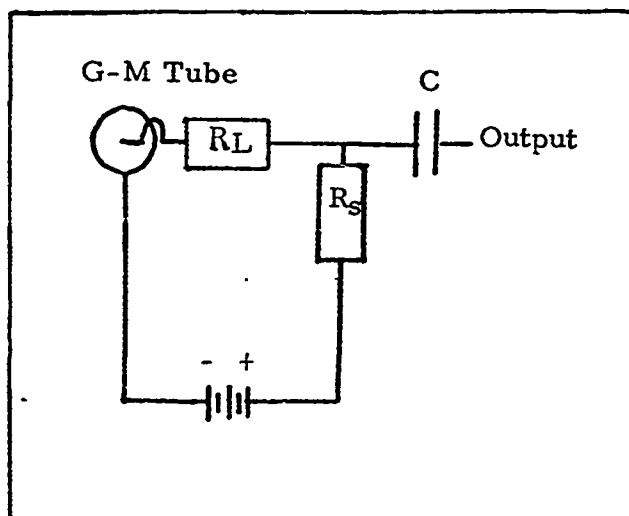


Fig. 2. The Fundamental Sensing Circuit Used in Experimental Testing

Even though only one capacitor is shown in the diagram, there are four different sources of capacitance: The G-M tube, the coaxial cable, the oscilloscope, and the listed capacitor. The G-M tube is composed of two concentric cylinders and thus produces a corresponding capacitance. The value of this capacitance was calculated to be 2.02 pf.

The second capacitance is derived from the length of the coaxial cable between the G-M detector and the sensing circuit. The cable used in this study has a value of 15-20 pf/ft.

The oscilloscope has a built-in capacitor when the AC position of the scope is used. This capacitance is in series with the scope input and has a constant value of 47 pf.

The last circuit capacitance is a  $0.05\mu f$  capacitor, that is also in series with the scope input. However, if the AC position of the scope is used, then this capacitor is not required and has no effect on the detected pulses.

The High Voltage Sources. As stated in the discussion of the sensing circuit, various high voltage (HV) sources were used in performing the experiments. All of these were off-the-shelf products and were employed in two methods: As a primary and as a secondary source. The primary source required a variable output from 0-2000 volts DC, and the secondary supplies were used to augment or "buck" the primary supply. The secondary supplies generally had a constant output of approximately 300 volts DC. The amount of secondary voltage input to the circuit (to "buck" or augment) was regulated via precision potentiometers.

Pulse Detecting and Recording Equipment. The Geiger pulses were observed on a Tektronix 535 oscilloscope using a type M plug-in unit. The "vertical output" of the scope was used to operate; a RJDL single channel analyzer and scaler-timer and a Tullamore count-rate-meter. These were used to

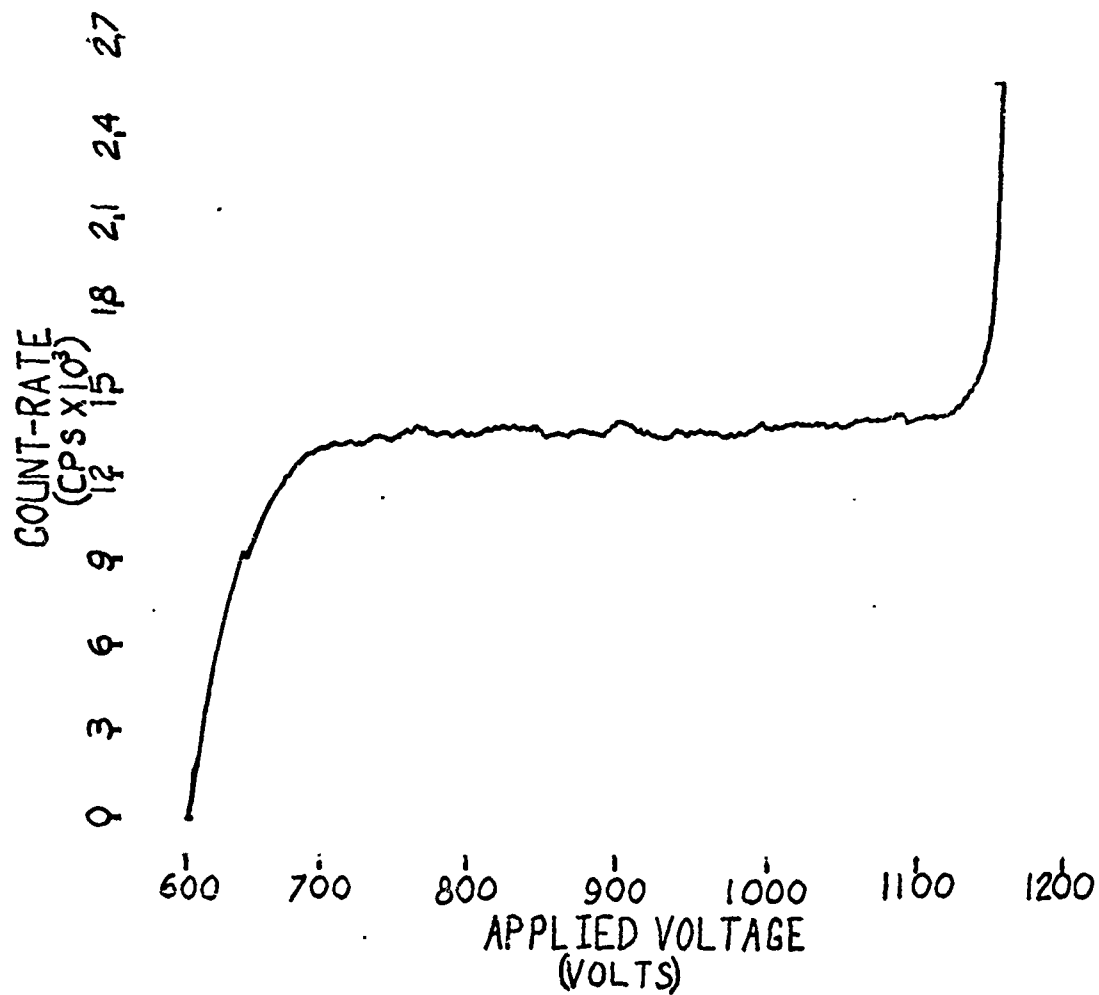


Fig. 3. Typical G-M Tube Plateau



count the pulses and also to plot plateaus of count-rate versus applied voltage.

The "plateau plotter" utilized a separate HV supply in conjunction with a 2000 volt operational amplifier. This combination enabled a voltage span to be swept horizontally along the X-axis of an X-Y recorder. The Y-axis of the recorder was connected to the output of the count-rate meter and thus, complete plateaus (as in Fig. 3) were made entirely automatically.

#### The Radiation Sources

The primary radiation source was 250  $\mu$  curies of  $\text{Cs}^{137}$ .  $\text{Cs}^{137}$  emits a  $\beta \sim 0.52$  MeV (maximum) and a  $\gamma = 0.66$  MeV. Two additional sources were used for the efficiency experiments;  $\text{Kr}^{85}$  and  $\text{Co}^{60}$ . Although  $\text{Kr}^{85}$  radiates both  $\beta$  and  $\gamma$  rays, the amount of  $\gamma$  radiation comprises a very small percentage (0.4 percent) of the total radiation. Therefore, a greater amount of it was used (4.0 curies).  $\text{Kr}^{85}$  has radiated energies of  $\beta \sim 0.67$  MeV (maximum) and  $\gamma = 0.54$  MeV.

The  $\text{Co}^{60}$  source has a much higher percentage of  $\gamma$  radiation, thus 200  $\mu$  curies were used. The radiated energy is in the form of  $\beta \sim 0.314$  MeV and  $\gamma = 1.17$  and 1.33 MeV (all listed radiations were taken from Ref 11:450-504).

#### IV. Experimental Tests, Procedures and Results

##### Introduction

It was stated in the introduction that the basic problem with the Nucleonic Oil Gauging System, is in the short life of the G-M tubes. Also, it was noted in theory, that G-M tubes fail because the halogen gas is lost due to reactions with the internal surfaces (most notably the cathode). With these facts in mind, it is the purpose of this section to ascertain answers to the following questions:

1. Do the aircraft G-M tubes age and fail because the halogen gas is being depleted?
2. If so, where does the loss of halogen gas occur?
3. Why does this loss occur?
4. Can this loss be reduced or eliminated?

With the answers to these questions as the goal, two environmental tests were performed:

Lifetime testing of G-M tubes in 200°C temperature and lifetime testing of G-M tubes in a combined environment (i.e., 200°C temperature and simulated aircraft vibrations).

In conjunction with the environmental tests, several analysis methods were performed on both new and failed tubes in order to determine any relative changes in the counter surfaces and/or gas composition. In the following list, the first three methods were used for surface analysis and the last two were used for gas analysis:

1. The Spark Source Mass Spectrometer,
2. The Auger Spectrometer,
3. The Scanning Electron Microprobe,
4. The Wet Chemical Gas Analyzer, and
5. The 21-491 Mass Spectrometer.

Further information on these methods is contained in Appendix C.

The two supplementary experiments were conducted in the areas of counter efficiency and vibrations, to gain the following information:

1. To find the variation in detector efficiency, with changes in cathode materials and dimensions,
2. To find materials which were basically halogen resistant, and
3. To find materials capable of withstanding the vibrations of the aircraft.

A preliminary analysis was made on a new tube, in order that relative comparisons could be made with aged and failed tubes from the environmental experiments. The results will be presented now, so that they will be available for use throughout this paper. The findings of the various analytical methods are listed in Table I, and summarized in the order in which they were listed above. Only two of these

Table I

## Results of the Analysis on a New Tube

Object Analyzed	Spark Source Counter	Auger Spectrometry	Scanning Electron Microprobe	Wet Chemical Gas Analysis
Cathode	-Negligible Br -Hydrocarbons main surface	-No bromine or Lead -Hydrocarbons (some)	-No bromine or lead -Hydrocarbons	
Surface Composition	- - Ni, Fe, Cr and spotty platinum	-Mainly Ni-O <sub>2</sub> definite quantities of Fe, Cr and small amounts of Pt. No Pb	- Layer of Pt - Layer of Ni - Cr -Fe base metal - Pt and Ni layers are cracked, and porous, with some Fe and Cr showing on surface - No Pb	
Anode	-Negligible Br	Thin layer of bromine	Thin uniform layer of bromine	
Gas Composition				108 $\mu$ gms of bromine (halogen)

methods (scanning electron microprobe, and the wet chemical gas analysis) approach quantitative results and so relative changes must be relied upon to draw conclusions.

#### Analysis of a New G-M Tube

The Spark Source Spectrometer Analysis: This method revealed traces of hydrocarbons and negligible amounts of bromine on the cathode. It also disclosed that the anode suffered an insignificant amount of bromine attack. The overall composition of the surfaces were very closely aligned with the manufacturer's patent (Ref 22:4); the only exception being the amount of electroplated platinum was not uniform and in some areas non-existent.

The Auger Spectrometer Analysis. Auger Spectrometry revealed no bromine on the cathode walls, however, the presence of hydrocarbons was fairly uniform. The primary composition of the cathode surface (from 0 to 200 Å) is nickel-oxide with small quantities of platinum, iron, and chromium present. Analysis of the anode did show a very thin uniform layer of bromine.

The Scanning Electron Microprobe Analysis. These results confirm those of Auger spectroscopy. The only differences were in the composition of the cathode. The microprobe revealed a definite layer of platinum on the surface and beneath this was layer of nickel. The platinum layer was by no means uniform and contained cracks, notches, and holes in which nickel, iron, and chromium could be detected.

The Wet Chemical Gas Analysis. If a new tube was filled according to the manufacturer's patent (Ref 22:4), then it should contain  $\sim 150 \mu$  gms of bromine. Results from this analysis revealed  $108 \mu$  gms were actually present. This deviation could be due to a lower total pressure (350 torr), lower halogen percentage (1.5%), or a combination of the two, but this quantity is considered to be within mass production limits.

The Mass Spectrometer Gas Analysis. The Mass Spectrometer was not used to sample the gases from a new tube, but was employed in the analysis of failed detectors and also several detectors, sent to the Air Force Flight Dynamics Laboratory from the "field".

Since little was known about the aging characteristics of the Harshaw geiger tubes, it was felt that a test in the simulated aircraft environment (i.e., both thermal and vibration) would not be immediately advisable. Instead, a test was first performed in a thermal environment where the complications of the vibrations were not present. This approach also gave considerable basic information on the aging characteristics of these detectors, which proved to be extremely valuable when the combined environmental testing was performed.

#### Lifetime Testing of G-M Tubes in 200°C Temperature

As was stated before, this experiment was performed to gain basic information on the aging

Table II

Results From the Thermal Environment Test  
General Surface / Gas Analysis

## Aging Characteristics

Tube	Method of Operation	V <sub>s</sub> Drop (volts)	Lifetime (hours)	Increased Lifetime via PHC	Object Analyzed	Spark Source Spectrometer	Wet Chemical Gas
1	Manual Pulse Height	116 *	190		Cathode	Bromine and Hydrocarbons	
2	Manual PHC	116 *	541		Anode	8.5 times more bromine per spot analyzed than the cathode.	
3	Manual PHC	174 *	1667				
4	V <sub>b</sub> = 700, R <sub>L</sub> = 5.1 MΩ	98 *	296	551	Cathode Surface Composition	Ni, Fe, and Cr with varying amounts of platinum	
5	V <sub>b</sub> = 700, R <sub>L</sub> = 5.1 MΩ	56 *	400	1082			
6	V <sub>b</sub> = 700, R <sub>L</sub> = 5.1 MΩ	145 *	379	1093	Gas		Three tubes Analyzed yielded: 9.5, 19, and 28.44 grms

\* For further information see Appendix D

14a

11-02/70/02-2

characteristics of the aircraft G-M tubes in a highly controlled temperature environment. The constant high temperature experiment was preferred to either a cyclic or ambient temperature test since the dissociated halogen species have higher reaction rates at elevated temperatures, and therefore this would constitute a "worst-condition" test.

Procedures. This experiment used six tubes divided into two tests. The first test consisted of three counters operated via manual pulse height control (i.e., the charge per pulse was controlled), where the applied voltage was always maintained below  $V_c$ . Since the reduced charge per pulse produces fewer energetic species (per pulse), the halogen gas has fewer excited species to quench (per pulse) and the end result should be an increase in lifetime for any given detector.

The second test was performed on the remaining three tubes, which were operated in the same manner as in the aircraft aging system. That is, each tube utilized a 5.1 M $\Omega$  load resistor and was operated at a constant 700 volts. When a detector failed, while operating in this configuration, its voltage was reduced to below  $V_c$  and the tube was operated under manual pulse height control. This was done to find whether the tube would rejuvenate itself or not, and if so, to determine what extension of lifetimes could be achieved.

Results. The results of this experiment are listed in Table II.

1. The Aging Characteristics. As indicated in Table II, the starting voltages dropped on every tube, as predicted. The drop-rate was approximately 45 volts/100 hours of testing, for the first 200 hours. This rate then decreased to below 7 volts/100 hours for the remainder of the experiment.

The changes in plateau shape were less well defined, but a pattern did develop and these changes will be discussed according to the modes of operation (i.e., with and without pulse height control). The starting points for the plateaus, of those tubes using pulse height control, reduced in voltage as  $V_s$  decreased. The plateau remained flat (2 percent increase in countrate per 100 volts change in potential) throughout the experiment. The most prominent indication of failure was when the detector became statistically unreliable as a "random event" counter. A very notable result of the experiment is that the average lifetimes of these tubes were twice those operated at a constant 700 volts.

The plateaus of the detectors operated at a constant 700 volts, had the same basic changes with  $V_s$ . However, as the tube aged, the upper end of the plateau (the multiple pulse region) decreased in voltage also. The tube would fail when the multiple pulse region coincided with the applied 700 volts. This tube would have to be replaced, at this time, if it were in an aircraft, but according to the procedures, the voltages were subsequently reduced below  $V_c$  and operation was continued using pulse height control. When this was accomplished, every tube rejuvenated itself and the average lifetimes were increased by a factor of between 3 and 4 (350-1200 hours). An explanation of this phenomena is that, as the tube

ages, the bromine content decreases. However, since the tube is operated at a constant 700 volts, the same approximate number of energetic species are created per pulse (with small changes due to pulse heights). This means that a smaller quantity of bromine must perform the same quenching processes and therefore, there is less time allowed for the dissociated species to recombine. The result is a rapid on-set of the multiple pulse region. Once the voltage is reduced, and the pulse heights controlled, the number of excited species per pulse is reduced, yielding more recombination time and thus, the rejuvenation of the detector's plateau and the extension of its useful lifetime.

It is indicated, by the changes in  $V_g$ , that the halogen gas is being depleted. In order to confirm this and to determine where the loss took place, two analysis methods were performed: The wet chemical gas analysis and the spark source mass spectrometer surface analysis. These will be discussed in the order listed.

2. The Wet Chemical Gas Analysis. Three tubes were analyzed for bromine content and each showed a significant decrease. The average bromine content was  $\sim 17 \mu$ gms as compared to  $108 \mu$ gms in a new detector. Thus, the loss of halogen gas is confirmed. Still unanswered is the problem of where this loss takes place.

3. Spark Source Spectrometer Analysis. The spark source mass spectrometer was used to analyze each of the three tubes and significant quantities of bromine were found on the internal surfaces and most notably the anode. The results show there was an average of 8.5 times more bromine (per spot analyzed) on the anode than on the cathode. The greatest amount of bromine attack still takes place on the cathode, since it has ten times the surface area, but the attack on the anode is significant. A literature search revealed little information about halogen attack on the anode or about the formation of negative bromine ions, which are the only known species that could accentuate the anode attack. However, it is plausible that a variety of highly active negative species are formed within the concentrated plasma discharge along the anode wire.

From this high temperature experiment, considerable detailed information has been gained on the aging phenomena of aircraft G-M tubes. However, the information is of restricted value since the total aircraft environment has not been duplicated. The basis has been laid and the results of the combined environmental experiment will be described next.

#### Lifetime Testing of G-M Tubes in a Simulated Aircraft Environment

With the knowledge that these G-M tubes age and fail because the excited halogen species attack the internal surfaces, a study of the additional effects caused by vibration should complete the answers of how and why these tubes fail so quickly in the aircraft.

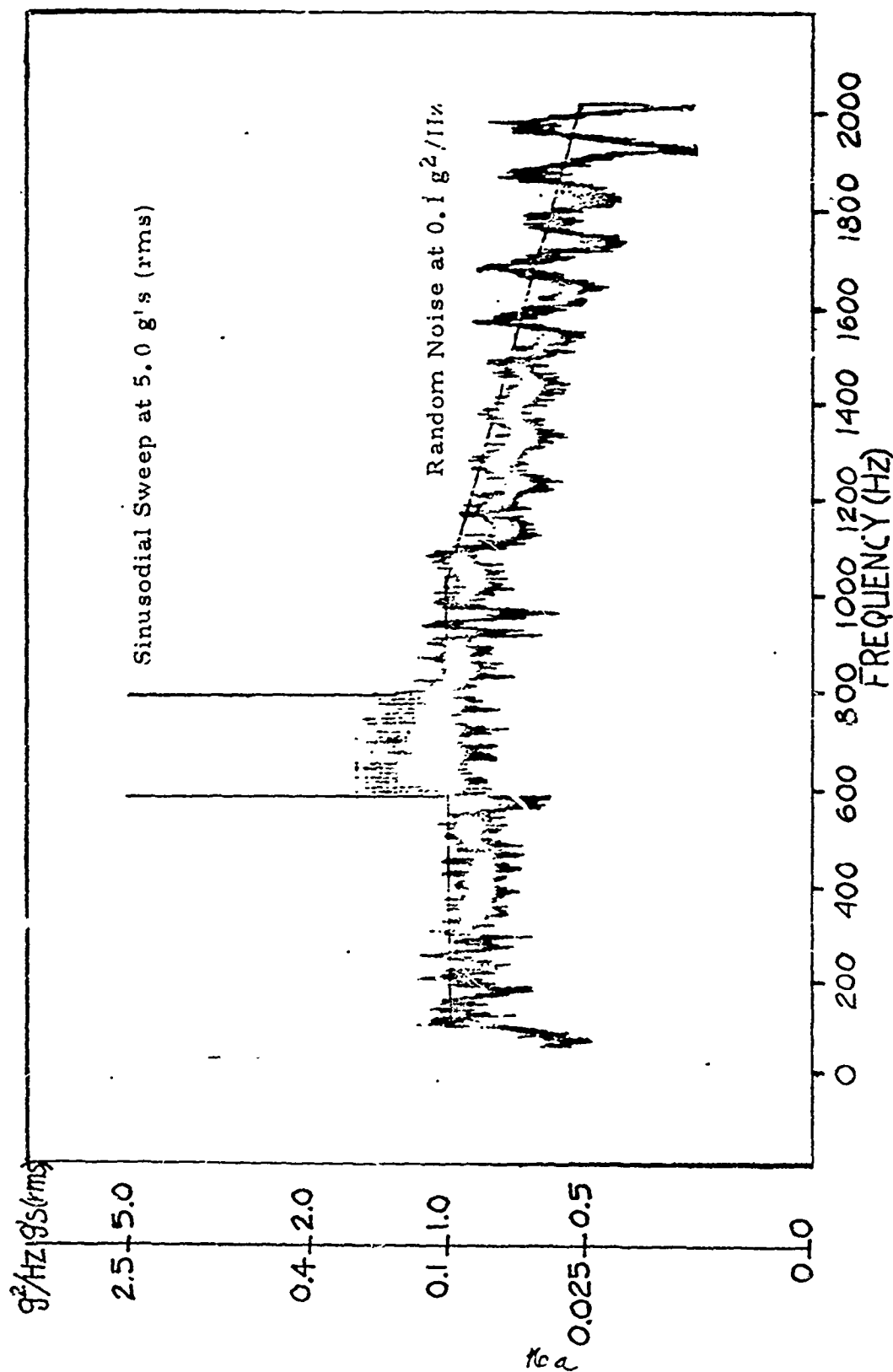


Fig. 4. Graph of Simulated Aircraft Vibrations



Procedures. The thermal portion of the experiment was conducted as before (i.e., the temperature was maintained at a constant 200°C). In order to simulate the vibrations of the engine, a tape of TF-41 engine vibrations (the engine used in the A-7D) was studied by the Combined Environments Branch of the Air Force Flight Dynamics Laboratory. Through this study a simulation was derived which consisted of two simultaneously operated components: A continuous random background noise and a sweeping sinusoidal wave. (A graph of the total simulated vibration is contained in Fig. 4). The random background noise was operated at  $0.1 \text{ g}^2/\text{Hz}$  and had 3db/octave "rolloff points" set at 100 Hz and 1500 Hz.

The sweeping sinusoidal wave covered the range of all the anode resonant frequencies ( $f_1$ ) and was operated at 5.0 g's (rms). The rate of the sweep was adjusted so that each anode was excited to its peak amplitude (at  $f_1$ ) during each sweep. Although this rate depends upon the spread in frequencies of the wires, for this experiment it was  $\sim 8 \text{ Hz/sec}$ . The overall advantages of this method of vibration testing are:

1. It is easy to reproduce,
2. It is more characteristic of all TF-41 engines than a tape, and
3. It can be used in batch testing.

A technical report will be written, at a later date, which will give the complete details of this mode of testing (Ref 4).

As in the thermal experiment, this test was also divided into two parts: Three tubes were operated with load resistors ( $5.1 \text{ M}\Omega$ ) and at a constant 700 volts and three tubes were operated with pulse height control. For the three PHC tubes, automatic pulse height controlling circuits (currently under development) were scheduled to be used, but because a "current leak" existed between the tubes and ground, the prototype circuits could not be utilized. Manual control (at potentials below  $V_c$ ) was also eliminated for the following reason: Because the amplitude of the anode wire was large at  $f_1$  ( $\sim 0.1$  inches), the field between the anode and the cathode increased greatly at  $f_1$  and, as a result, even with potentials below  $V_s$ , the pulse heights would be large and more characteristic of those above  $V_c$ . In essence, little control of the charge per pulse was being obtained. Thus, another method had to be found and since the amount of charge in an "uncontrolled" pulse is  $\sim 9000 \text{ p coulombs}$  and the charge in a "controlled" pulse is only  $\sim 70 \text{ p coulombs}$ , it was decided that the effect of a "perfect" controlling circuit could be simulated by operating the detectors with no applied voltage (i.e., no charge per pulse).

The sequence of pictures shown in Fig. 5, 6, and 7, depict the pulses of tubes using; no pulse height control (Fig. 5), manual pulse height control below  $V_c$  (Fig. 6), and the automatic pulse height controlling circuit (Fig. 7). The circuit used to produce the effect in Fig. 7, is presently under investigation and development by the Air Force Flight Dynamics Laboratory under the direction of Captain

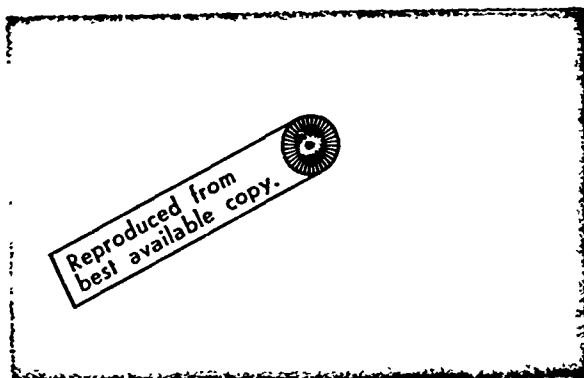
1.5  
 $\frac{V}{cm}$



$10^{-3}$  Sec/cm

Fig. 5. Geiger Pulse - - No Pulse Height Control

0.15  
 $\frac{V}{cm}$



$10^{-3}$  Sec/cm

Fig. 6. Geiger Pulse - - Manual Pulse Height Control  
With  $V_B < V_c$

0.15  
 $\frac{V}{cm}$



$10^{-4}$  Sec/cm

Fig. 7. Geiger Pulse - - Automatic Pulse Height Control

R. P. Couch. The same procedure was used as before, when a tube operating at a constant 700 volts failed (i.e. it was subsequently operated using pulse height control) or, as will be explained later, the voltage would be removed entirely. Again, it was desired to ascertain if the tubes would rejuvenate themselves and if so, what extensions to their lifetimes could be gained.

Results. The tabulated results in Table III contain the aging data and the general surface and gas analyses. These results confirm those found in the thermal experiment and also give considerable insight into the factors leading to the depletion of the halogen gas. The following summary discusses each of the results listed in Table I and in the following order: aging characteristics, surface analyses, and gas analyses.

1. The Aging Characteristics. The aging characteristics of these six tubes followed the same pattern as in the thermal experiment, with the most notable factor being a drastic increase in the rate of aging. Also, for the first time, the last known aging characteristic, oscillations, was detected. These characteristics will be discussed as before (i.e., changes in  $V_s$ , then changes in plateau) with the electrical oscillations being last. As in the thermal experiment, every tested detector showed considerable decreases in  $V_s$ , the main difference being the rate of change. In the thermal environment this rate was 45 volts/100 hours and less for the entire test, however, in this experiment the rate was 600 volts/100 hours for the first 30 hours of testing. Although the test was concluded prior to the complete failure of all tubes, the "best" detector showed a loss of 150 volts and the "worst" tube failed in only 6.0 hours (see Table IIIA). It should be noted that at the end of the 53 hours, three of the six detectors had failed in one form or another.

Basically, the changes in the plateaus were the same as those in the thermal experiment with the most notable difference again being the increased rate. The failure indications were also similar, except that the detectors aged so rapidly that no real changes were noted in their counting accuracy before they failed completely. By examining the two different modes of operation, a better viewpoint on their plateau changes can be gained. Those tubes using pulse height control, showed the same changes as in the thermal experiment and they also had twice the average lifetimes of those operated at a constant 700 volts. The plateaus of all the tubes had a slope of  $\sim 2.0$  percent/100 volts, and this increased to 5.0 percent/100 volts at the conclusion of the experiment. However, just prior to failure the count-rate-increase could be as large as 10 percent/100 volts.

The counters operated at a constant 700 volts had the same general changes and percentages. Two of these detectors failed before the test concluded and then continued their operation using pulse height control. Only one of these two tubes rejuvenated and it continued operating successfully until the end of the experiment. In essence, the pulse height control extended its life by a factor of 8

Table III A

## Results From the Combined Environment Test

## Aging Characteristics

Tube Number	Method of Operation	Total $V_s$ Drop	Lifetime (hours)	Lifetime Extension via P.H.C.
1	P.H.C. *	280 **	51.0	
2	P.H.C. *	150 **	53.0	
3	P.H.C. *	280 **	31.5	
4	$R_L = 5.1 \text{ M}\Omega$ and $V_B = 700 \text{ volts}$	194 **	6.0	49.0
5	$R_L = 5.1 \text{ M}\Omega$ and $V_B = 700 \text{ volts}$	214 **	53.0	
6	$R_L = 5.1 \text{ M}\Omega$ and $V_B = 700 \text{ volts}$	321 **	18.2	

\* PHC = Pulse Height Control

\*\*For further information see Appendix D

Table III B

## Results From the Combined Environment Test

	General Surface/Gas Analysis		
	Spark Source Spectrometry	Auger Spectrometry	Scanning Electron Microprobe
Surface			Wet Chemical
Cathode	-Pt, Br, Pb, and Hydrocarbons	-Uniform Br layer -Hydrocarbons and Pb in small quantities	-Br co-located with Pb, no uniform layer -Hydrocarbons
Anode		-Uniform Br layer, Thicker than on new wire	
Abrased Anode	Strong Br, FeBr, and PbBr and slight NiBr returns. -Pb and Hydrocarbons	-Less Br on abraded spot than towards longitudinal center	
Cathode Surface	Fe, Cr, Ni, and Pt	-NiO <sub>2</sub> mostly, some Fe and Cr. -No Pt down to 200Å depth.	-5m thick Pt layer not uniform, has holes and cracks. -10 m thick Ni layer -Remainder Fe and Cr.
Gas Analysis			(1.0M gms per tube

(see Tube #4, Table I). Although this is significant, it must be realized that the experiment only lasted 53 hours and thus even the pulse height controller cannot compensate for inadequate designs or materials.

The last area of the aging characteristics, is the electrical oscillations. This phenomena occurs at very low percentages of halogen gas and in the case of these detectors, this quantity was less than 1.0  $\mu$ gms. An explanation of this phenomena and three examples of oscillations are contained in the works of Usacev (Ref 30:43). All three of the reported oscillations were noted in this experiment and one new example as shown in Fig. 8. This oscillation was peculiar because of the "damping" effect noted after every 2-3 cycles.

Another point of interest is that there was a definite sequence, in which the various oscillations were

V  
O  
L  
T  
S

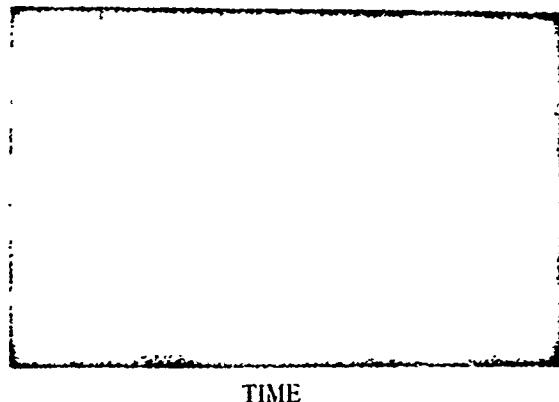


Fig. 8. "Damped" Oscillations

detected. Although every step in the sequence involved a continuous oscillation, the frequency ranged from  $\sim 15$  Hz to 40 Hz and the amplitudes varied between 0.02 volts and 0.3 volts.

The results of the surface analyses for this experiment are extremely interesting and important. In order to present these in a clear and precise manner, each method will be discussed in the following order: Spark source mass spectrometry, Auger spectrometry, and scanning electron microprobe. There is one result that should be noted first; on the anode of each failed tube, an abraded spot was found which corresponded to the edges of the ceramic insulators. The depth of this spot varied between different wires, but it was clearly visible to the unaided eye on every wire. Another connected side-light of interest, is a test that was performed on both a Harshaw and a Techniques Geiger Muller (TGM) tube. This experiment entailed vibrating each tube at the anodes'  $I_1$  and at 20 g's (rms). According to military specifications (Ref 21:13), this test was to last at least one hour, with negligible changes in the tested detectors. The Harshaw tubes' anode broke after  $\sim 15$  seconds. The TGM tube failed after  $\sim 20$  minutes. In both cases the "break" occurred at a point corresponding to the ceramic insulators. This signifies that severe abrasion is taking place at 20 g's, and implies that the test is too strenuous and/ or the detectors are below the required quality. At any rate, this spot was examined closely by the spark source counter and Auger spectroscopy. An examination via the scanning electron microprobe is also under way but the results were not gathered as of this writing.

2. The Spark Source Spectrometer Analysis. Investigation via spark source spectroscopy revealed that definite quantities of bromine (Br), lead ( $Pb$ ), and various hydrocarbons existed on the internal surfaces, and so to make sure that all the information is presented, the cathode and anode surfaces will be discussed in turn. The cathodes showed the same basic materials as before (i.e., Pt, Ni, Cr, and Fe), but also present in significant quantities were bromine and lead. As of this time, however, no actual bromides have been found.

The results for the anode were considerably different especially in the areas around the abraded spot. In these areas the basic material was detected (Cr, Ni, and Fe) but more than this, bromine was found in very high concentrations. Also present in significant quantities were iron bromide, lead, lead bromide, and numerous hydrocarbons (e.g.,  $C_4H_9$ ,  $C_7H_{11}$ ,  $C_7H_{13}$ ). A small trace of nickel bromide was also present but this was extremely small as compared to the other bromides.

3. Analysis by Auger Spectrometry. Auger spectroscopy confirmed the presence of bromine on the cathode and anode. Shots made at numerous places along the cathode revealed a uniform bromine layer and small quantities of lead. The basic cathode materials were the same as those listed in the analysis of a new tube (see page number 14).

In analyzing the anode, emphasis was placed on the abraded spot. A thorough examination revealed that less bromine was present on the spot than on areas closer to the longitudinal center of the wire. Although this appears to conflict with the results of the spark source counter, the correlation lies in the way the two different tubes failed. The tube analyzed by the spark source counter did not totally fail prior to being removed from the experiment, however it had shown a considerable degradation in performance. Since the halogen gas was not totally depleted, it continued to react with the abraded spot and built up a considerable deposit. Contrary to this, the tube examined by Auger spectrometry, totally failed while remaining on vibrator. Thus the wire was continually rubbed clean and therefore less bromine should be (and was) detected on this spot than towards the longitudinal center.

4. The Scanning Electron Microprobe Analysis. The last surface analysis was made via the scanning electron microprobe and again definite formations of bromine on the cathode and anode were evident. Up to this time it had been suspected that the bromine was attacking the platinum surface or the iron through the holes in the platinum layer. The microprobe results showed that the bromine was always co-located with lead deposits and vice-versa. For the first time a definite combination for surface attack on both the cathode and anode was confirmed (Pb Br). A sequence of photographs showing a cross-section scan of the various materials that make up the cathode walls are in Figs. 9,

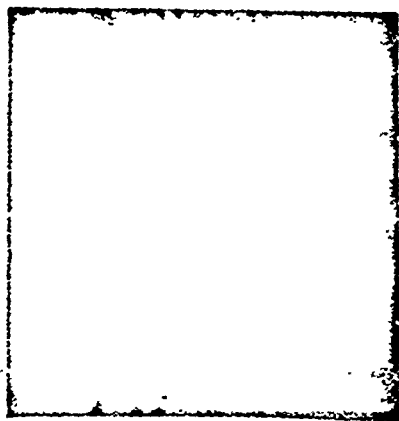


Fig. 9. Cross-section Scan  
of Cathode for Pt

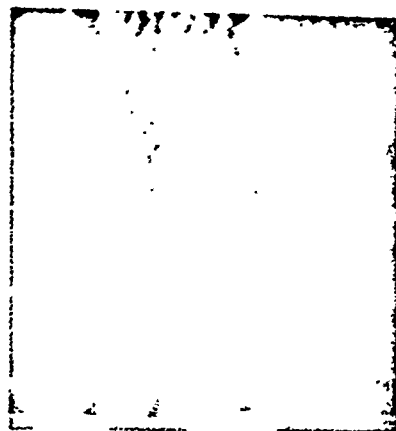


Fig. 10. Cross-section Scan  
of Cathode for Ni



Fig. 11. Cross-section Scan  
of Cathode for Fe

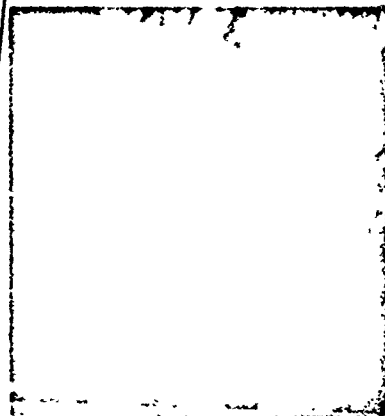


Fig. 12. Cross-section Scan  
of Cathode for Cr

Reproduced from  
best available copy.

In each of the figures above, a line-scan was taken to find where the concentration of Pt, Ni, Fe, and Cr was located. The inner surface of the cathode is just to the right of the black vertical line. The remainder of the cathode goes off the picture to the right. As can be seen, Pt is the first layer and then Ni. The remainder of the cathode is basically Cr-Fe.



10, 11, and 12. The other two figures (13 and 14) show a lead spot and an x-ray scan for bromine on that spot (the bromine is located in the brightest groups on the dark spot of lead).

Microprobe results revealed that significant bromine attack occurred on the anode. However, contrary to spark source counter results, no lead was detected. Recall that when a new wire was analyzed, a thin uniform bromine layer was present; however, that analysis was made using 10 KeV electrons. On the other hand, the scans made for bromine on this wire utilized 30 KeV electrons, which implies a more penetrating bromine attack. There was no uniform layer at this depth but there were considerable areas of attack (see Fig. 15). Although an abraded wire has not yet been analyzed by this method, the arrangements have been made to do so. Unfortunately, the results were not available prior to the writing of this paper.

The question arises here as to where the lead comes from and how it disperses itself throughout the chamber. The total answer is not known, but the only source of lead in the tube is from the solder glass (which is basically a lead oxide). It was forwarded that the lead contamination occurred during the curing cycle, and if this is true, lead should be present in new tubes. However, examinations of new tubes failed to reveal the presence of lead (see Table I). Therefore, this is not likely to be the mechanism by which lead contamination takes place. Another possibility is that the lead is drawn out of the glass by a combination of continuous heat and the increased electric fields caused by the vibrations.

There is no doubt that at temperatures above 100°C, lead and lead oxides are attacked by bromine (Ref 29:213). It appears that basic changes in materials

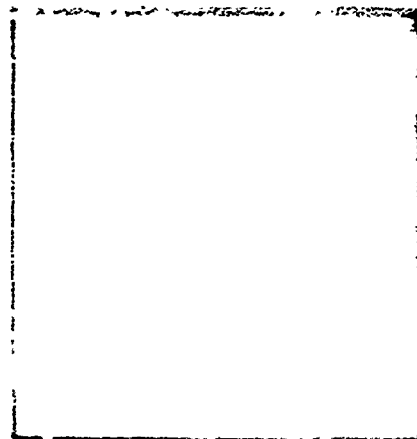


Fig. 13. Lead Spot on Cathode

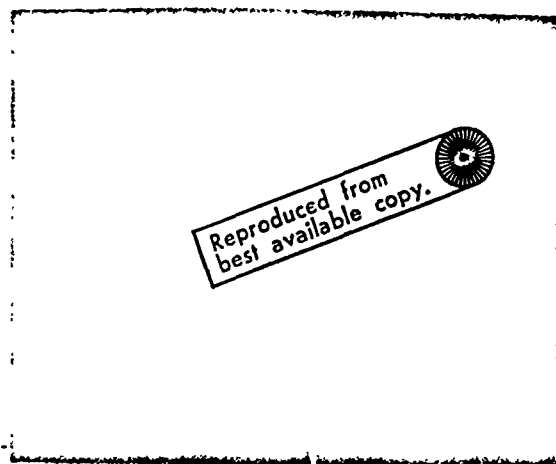


Fig. 14. x-ray Scan of the Lead Spot (Fig. 13) for Bromine



Fig. 15. Bromine Attack on the Anode

and design will be required if a truly "rugged" detector is to be built.

The last area in this results section is the analyses made on the gas within the failed counter. Two methods were used and will be discussed in the following sequence: Wet chemical gas analysis and mass spectrometer analysis.

5. The Wet Chemical Gas Analysis. The findings of the wet chemical gas analysis are short, but significant. In every failed detector, there was less than 1.0  $\mu$ gms of halogen gas.

6. The Mass Spectrometer Gas Analysis. The 21-491 mass spectrometer was used for this analysis and was equipped with a sample inlet system especially designed for this study. Several tubes from the "field" were analyzed as well as one from this experiment. The results indicate that bromine, chlorine, iodine, cyanogen bromide, and carbon dioxide were present in each of the tubes analyzed along with the basic compositions of neon and argon. It was suspected that hydrocarbons would also be detected, since they were found on the internal surfaces. However, none of the tubes analyzed contained detectable amounts of hydrocarbons.

### Summary

As a result of these two experiments, the first two questions are satisfied: The tubes fail because the halogen gas is depleted and this depletion is due to reactions with the internal surfaces. The important factor though, is not that the bromine reacts with the surfaces, but which surfaces and how. These questions are also answered i.e., the cathode is attacked due to lead (or lead oxide) deposits and the anode because:

1. Its basic composition is not halogen resistant, and
2. The abraded areas continue to reveal new surfaces for attack.

Thus the third question as to why the loss occurs is also answered.

The focus is now turned to the final question: Can the loss of halogen gas be reduced or eliminated? By using halogen resistant materials capable of withstanding the aircraft environment, it is felt that the loss of halogen gas (through reactions) can be reduced and/or eliminated. But three questions immediately present themselves:

1. What halogen resistant materials can withstand high temperatures ( $\sim 200^{\circ}\text{C}$ )?
2. What effect will these materials have on the detector's efficiency?
3. What materials will be capable of withstanding the aircraft vibrations?

These questions require considerable investigation in order to determine how the detector should be changed. Thus the two supplementary experiments were performed, namely determining the efficiency of various cathode materials and dimensions and determining the ability of these materials to withstand aircraft vibrations. It was expected that, the addition of these results to those gained from the environ-

mental experiments would constitute a solid foundation, from which recommendations for a truly "rugged" G-M tube could be made. These supplementary experiments will be discussed in the order in which they were introduced (i.e., the efficiency and then the vibration test).

### The Efficiency Experiment

Introduction. This study was undertaken to better understand the interrelationships of the variables that enter into the efficiency of a G-M tube (e.g., counter dimensions and materials). When discussing efficiency two different definitions are encountered. The first form deals with the probability that a given material will emit an electron, while being bombarded by some constant radiation field. The second form is the probability that this freed electron will initiate a discharge and be collected on the anode. In almost all G-M counters, the second form is greater than 99 percent (Ref 16:27). Therefore, only the first definition is dealt with in this experiment.

As was noted in the theory section, the efficiency of electron production is effected by the photon energy, the cathode atomic number ( $Z$ ) and the density of the traversed media. It was also concluded that the greatest majority of the free electrons are generated in the cathode. In general, the higher the atomic number, the greater is the probability of electron production. This is based upon the primary mechanisms for electron production in the cathode (i.e., photoelectric and Compton effects). The dependance of these effects upon  $Z$  and  $h\nu$  are expressed in their cross-sections by Price (Ref 25:25, 27), as:

$$\tau = f \left[ \frac{Z^5}{(h\nu)^{3.5}} \right] \quad (2)$$

for the photoelectric effect and

$$\sigma = f \left[ \frac{Z}{(h\nu)} \right] \quad (3)$$

for the Compton effect. Therefore the ratio

$$\frac{\tau}{\sigma} = f \left[ \frac{Z^4}{(h\nu)^{2.5}} \right] \quad (4)$$

shows a strong dependance on both the atomic number and the energy of the photon. The type of material is also important when determining the optimum thickness for the cathode. Von H. Gebauer (Ref 31:138) found that the relationship between photon energy, atomic number, and optimum thickness obeys the equation:

$$d_{opt} = \frac{2.3(h\nu)^{1.22}}{Z^{1.14}} \text{ cm} \quad (5)$$

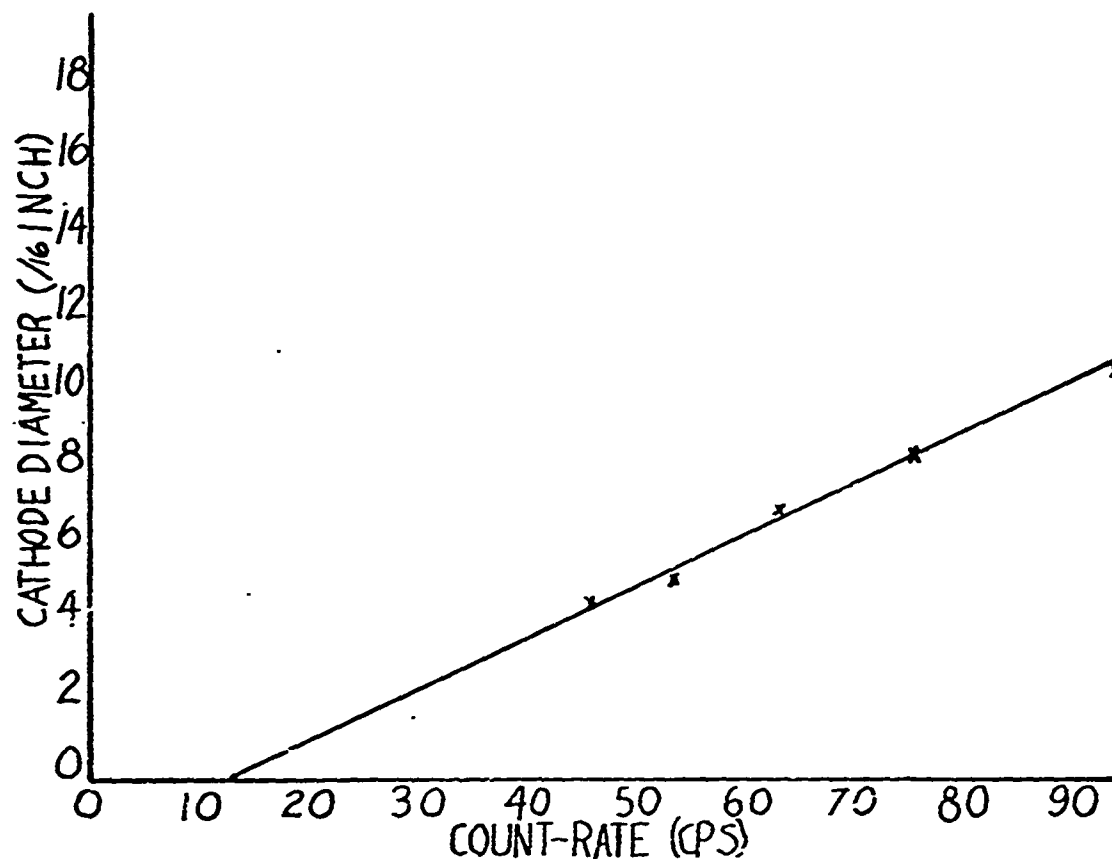


Fig. 16. Efficiency vs Cathode Diameter

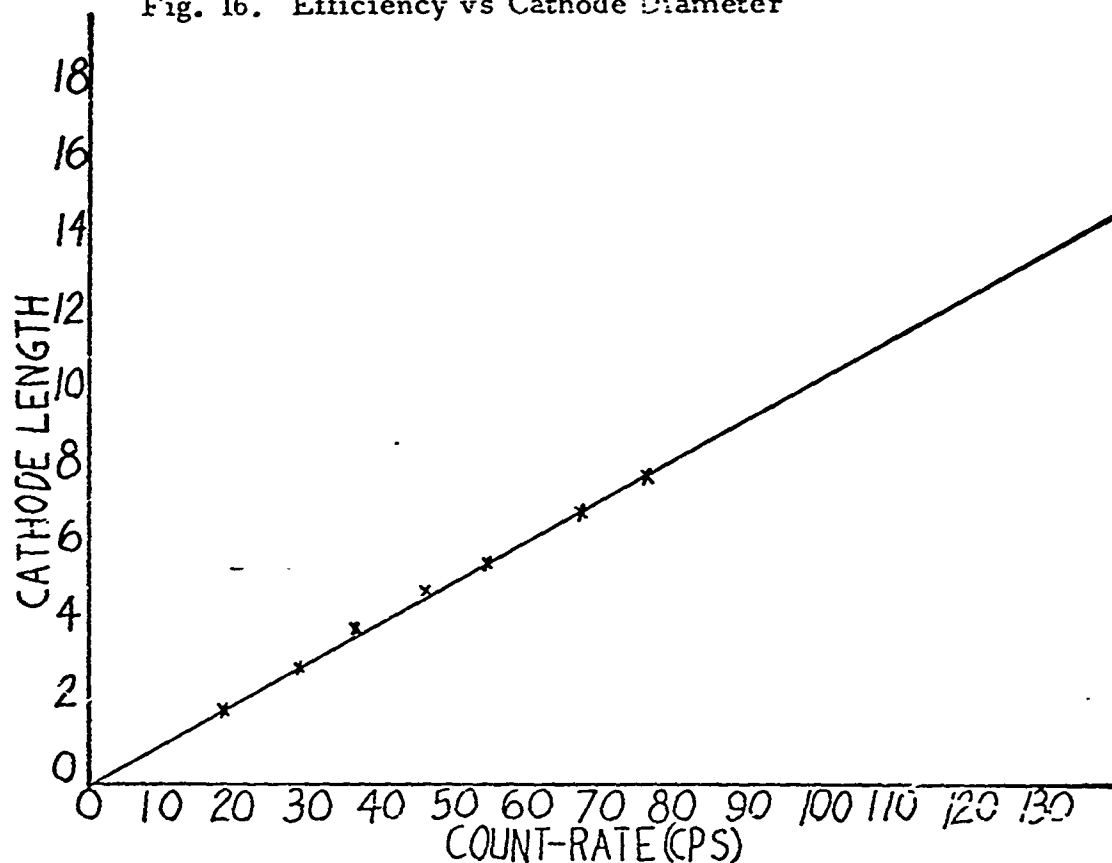


Fig. 17. Efficiency vs Cathode Length

Thus, even though no one equation is available to determine the exact efficiency of a given tube, a very good indication can be gained by simply examining the radiation source and the cathode material. However, more precise information is desired in order to determine trade-off points for designing the best possible tube. One example of these trade-off points would be increasing the volume-to-surface ratio of the tube. If efficiency is not impaired, then a larger volume-to-surface ratio would result in a proportionately greater volume of "quenching" gas with smaller amounts of "reacting" surface (if a constant total pressure is maintained). This should result in a detector with a longer lifetime. Hence, efficiency experiments were performed, and since efficiency is controlled by the cathode dimensions and material (atomic number) the experiment was subdivided into two tests covering each of these areas in turn.

#### Procedures.

1. Efficiency vs Counter Dimensions. It would probably be more meaningful to refer to this experiment as a controlled study of efficiency by varying the surface to volume ratio. Since the primary factors in the surface and volume formulas are diameter and length tests were performed on tubes having a variety of lengths and diameters.

Both of these tests utilized: 250  $\mu$  curies of  $C_{54}^{137}$ , a 3.1 mil nickel anode, and Q-gas. The cathode was 4 inch copper tubing (in the first experiment) and the diameters ranged from 7/16 inch to 17/16 inch. The detector was operated as a flow-through counter having entry and exit ports on opposite ends of the counter. With each new cathode arrangement, a complete plateau was taken and the time required to accumulate  $10^4$  counts at some point on the plateau was recorded.

The second part of the surface-to-volume test was conducted in a similar manner except the material used was aluminum and its diameter was constant at 7/16 inch. The lengths were varied from two inches to seven inches in one inch increments and the same data gathering processes were followed as before.

2. Efficiency vs Cathode Materials. The second portion of the efficiency experiment dealt with changes in cathode materials. The different materials studied were: Ni, Pt-10Ir, Hastelloy C-276, 302 stainless steel, copper, two different E-C coatings on glass, and aluminum, all in four inch lengths. With each cathode material, the same anode and fill gas was used (i.e., 3.1 mil nickel and Q-gas) as before. Three different sources were used in order to get an energy spread ( $Kr^{85}$ ,  $C_{54}^{137}$ , and  $Co^{60}$ ), and the same data gathering techniques were followed.

Results. From the surface-to-volume experiment it was found that the efficiency varies linearly with both length and diameter as shown in Fig. 16 and 17.

The effects of changing cathode materials were not nearly so clear cut. However, one definite result was that the efficiency is less atomic number dependent with higher  $\gamma$  energies. This is exemplified by the fact that there is very little difference in efficiency between all the materials tested

when  $\text{Co}^{60}$  was used. Contrary to this, Pt-10Ir was more than twice as efficient as any of the other materials when  $\text{Kr}^{85}$  or  $\text{Cs}^{137}$  were used. Since  $\text{Kr}^{85}$  is the source used in the aircraft, it appears that counter designs should consider using a high Z material, provided it is non-reactive with halogen gases.

Summary. This summary is set forth to gather the results which have been discussed to this point before continuing the discussion:

1. The tubes age and fail due to a loss of halogen gas.
2. The loss of halogen gas is due to reactions with the inner surfaces of the detector.
3. The reactions are due in part, to the presence of impurities such as lead and hydrocarbons.
4. The vibrations cause worn areas on the passivated anodes which also results in significant halogen attack.
5. The efficiency of a G-M counter varies linearly with its length and diameter.
6. The efficiency is more dependent upon cathode material when lower energy sources are used.

The total solution, however, must involve a definition of:

1. Materials not reactive with halogen gases.
2. Materials that yield high efficiency.
3. Materials that yield high strength under vibration.

These factors will be discussed next.

A detailed tabulation of materials properties as they relate to halogen attack is found in Appendix B. From this analysis it is concluded that "Elinvar Extra" and possibly E-C coated glass could be used as improved materials. The last area to be considered is the vibrational characteristics of various materials.

### The Vibration Experiment

Introduction. In the analysis of the taped engine vibrations, it was found that, if the fundamental frequency of the anode could be raised above 2000 Hz, the major portions of the engine vibrational-energy-input would be avoided. The fundamental frequency can be determined by the following equation:

$$f_1^2 = \frac{T}{4\ell^2 p A} (\text{Hz})^2 \quad (6)$$

where T is tension,  $\ell$  is the unsupported length,  $p$  is the material density, and A is the cross-sectional area of the wire. As can be seen, the main factor is the unsupported length, however, if the length is held constant, the ultimate tensile strength for a given wire dictates whether it can be used or not.

This test was conducted to find what anode materials would physically be capable of enduring the vibrations within the aircraft. Although there are many materials available, there are also many different factors that must be satisfied such as: Halogen resistance, ultimate tensile strength, and matching coefficients of expansion. As a matter of fact, one of the largest problems in modifying the present

counter design, is matching the expansion coefficients. In this endeavor, a maximum acceptable deviation, is  $\pm 1.0 \times 10^{-6}/^{\circ}\text{C}$ . for all the counter materials. Therefore, even though this experiment deals only in the vibrational characteristics for the anode, it necessitated a detailed study of many different materials for use as cathodes, anodes, insulators, and sealants.

This study revealed that the most halogen resistant material at high temperatures, is nickel (Ref 29:682). However, there are others that can be used and so the following materials were tested: 304 hard stainless steel, Pt-10Ir, Pt-10Rd, Elinvar Extra, Hastelloy C-276, Ni, and Ni-2Be. Details of composition, ultimate tensile strength, density, coefficient of expansion and halogen resistance are contained in Appendix B.

Procedures. This experiment consisted of testing the various wires at many different tensions up to and including their ultimate tensile strengths. The lengths of all the wires were constant at 2.38 inches but the cross sectional area depended upon the individual wire sample (this varied from 5-30 mils). With each sample and tensile strength, the fundamental frequency was recorded. After several readings were taken at different tensile strengths, an endurance test was conducted. The endurance test consisted of vibrating the given wire (at a constant length) at  $f_1$  until the wire failed or it attained  $10^8$  cycles. It was felt that if the wire endured  $10^8$  cycles at  $f_1$ , then for this configuration, the wire would mechanically last indefinitely.

Results Tensile tests showed that every material, except 304 "full hard" stainless steel, failed at a tensile strength well below their rated-ultimate tensile strengths. This could have been caused by side loading stresses being placed on the wire by the mountings, or a defect in the wire material. The highest fundamental frequency recorded in the vibration experiment was 3586 Hz by the stainless steel sample but unfortunately, the halogen resistance of 304 stainless steel is poor. The primary purpose in testing it, though, was for use as a comparison. Both the platinum alloy wires, were too soft, and stretched beyond all practical use during the vibrations. Of all the halogen resistant materials tested, a preferential listing (according to their vibrational characteristics) would be: Nickel-beryllium, Hastelloy C-276, Elinvar Extra, nickel and then the platinum alloys. Details of these materials and a comparison of calculated versus actual  $f_1$ 's are contained in Table IV in Appendix B.

### Summary

This section completes the discussion of the experimental portions of this thesis. A review of exactly what the desired goals were and what has been accomplished toward those goals is given below.

The goals were listed in the introduction as the following questions:

1. Do the aircraft G-M tubes age and fail because the halogen gas is being depleted?
2. If so, where does the loss of halogen gas occur?
3. Why does this loss occur?

4. Can this loss be reduced or eliminated?

In answer, the following statements are made:

1. Yes, the aircraft G-M tubes do age and fail because the halogen gas is being depleted.
2. This loss occurs due to reactions with both the anode and the cathode.
3. This loss occurs in general because of: Poor materials (anode and sealing glass), impurities within the chamber (lead and hydrocarbons), and poor vibrational design.
4. Since the losses are due, for the most part, to materials, equipment and design, is it felt that these losses can be at least reduced, if not totally eliminated.

This paves the way for the final section of this thesis: Conclusions and Recommendations.



## V. Conclusions and Recommendations

The previous portions of this thesis have been dedicated to experimentally determining why and how the aircraft G-M tubes fail so rapidly. Considerable information has been gathered and analyzed so that this final section can forward conclusions and recommendations based on solid facts. Thus the last portions of this thesis are, in essence, the "fruits-of-labor".

### Conclusions

There are a number of conclusions that can be drawn from this study. These conclusions are divided into two groups as were the experimental tests. That is, conclusions will be drawn first from the environmental, and then from the supplementary experiments.

From: the Environmental Experiments. These conclusions are concerned primarily with the aging phenomena, causes for the detector failure, and the effects of different modes of operation and are numerically listed for simplicity and completeness.

1. The detectors age and fail in accordance with known aging phenomena. That is,  $V_s$  decreases with age, the plateau starts and ends at lower voltages and its slope increases with age, and oscillations are detected when the halogen content is very small.
2. The detectors fail because the halogen gas is depleted.
3. This loss is due to reactions with the cathode and anode.
4. These reactions are caused by: Impurities in the G-M tube, use of materials that give rise to impurities, and materials that are not basically halogen resistant.
5. The rate of these reactions is increased by the abrasions on the anode caused by the vibrations.
6. The use of a pulse height controller reduces this rate by allowing less charge (and hence, less active species) to be generated per pulse.
7. The pulse height controller increases the lifetime of a detector at least by a factor of two.

From the Supplementary Experiments. This sub-section sets forth conclusions concerning efficiency and vibrations of various counter materials and dimensions. Again, the conclusions are numerically listed.

1. Detector efficiency varies linearly with length and diameter (or with the surface area).
2. Efficiency is atomic-number-dependent primarily at low energies.
3. Low efficiency can be compensated for, by using larger and stronger sources or larger surface area detectors.
4. In order to achieve  $f_1$ 's greater than 2000 Hz, shorter anode lengths ( $\sim 3''$ ) are necessary.

5. In order to prevent anode abrasions, wider insulators are required, because the fundamental frequencies cannot be increased (under present counter design) and thus the amplitudes cannot be reduced.

The next step is to forward recommendations which will satisfy the final goals of this thesis: To modify the present detector in order to yield a longer life and/or to develop a truly "rugged", long life G-M tube.

### Recommendations

The problems caused by the short-lifetimes of the aircraft G-M tubes, are very pressing and immediate remedies are required. However, the truly "rugged" long life G-M tube will require further studies and so this section is divided into three sub-sections: Immediate modifications, interim changes and recommendations for further investigation.

Before continuing, there is one general recommendation which requires no change in the present system, yet it will (at the very minimum) double any detectors life time: The use of the pulse height controller. The use of this circuit is recommended regardless of what G-M tube design is utilized.

Immediate Modifications. The recommendations forwarded here will require a minimum of detector changes in order to achieve the maximum in lifetime extensions. The recommendations are listed and discussed as follows:

1. Replace the anode with a more halogen resistant material.
2. Increase the internal diameter of the insulators, so that anode abrasions will be reduced.
3. Investigate the materials, equipment, and procedures used in detector production.

The various surface analyses prove that considerable amount of bromine is absorbed on the 17-7 PH anode wire and, therefore, it should be replaced. Elinvar Extra is recommended because it has a high nickel content (43 percent) and high nickel alloys are known for their halogen resistance. Another reason for recommending Elinvar Extra is that its coefficient of expansion matches the other materials presently used.

The anode abrasion problem can be reduced by several methods, but increasing the internal diameter of the forsterite insulators requires the least amount of detector modification.

The presence of impurities (hydrocarbons and lead) on the counter surfaces, implies that insufficient care is being exercised in the selection and processing of the various materials used in the detector. As stated before, the only known source of lead, inside the tube, is from the glass solder, and the hydrocarbons most commonly arise from dirty vacuum systems or improperly trapped diffusion pumps. It is strongly felt that an investigation into the materials, equipment, and procedures, used in detector

production, is warranted and necessary.

Utilizing these recommendations, combined with the lifetime extension of the pulse height controller, the minimum time between failure should be increased to ~1000 hours or more.

Interim Changes. The recommendations of this section will require basic changes in the counter dimensions and thus requires more time to implement. Also, these recommendations assume that the suggestions from the previous section have been adopted. With this in mind the following two recommendations are made and explained:

1. Increase the detectors volume-to-surface ratio, and
2. Decrease the detectors overall length.

As was noted in the introduction to the efficiency experiment, an increased volume-to-surface ratio means that more quenching gas is available to react with a proportionately smaller surface area. Therefore, even if the present materials were used, a longer lifetime should be gained. However, the best method of increasing the volume-to-surface ratio is to increase the diameter of the cathode. Thus there is more room in which a larger insulator could be used and if so, this will reduce the possibility of anode abrasion.

The second recommendation calls for a reduction in both the cathode and anode lengths. This will cause the anodes'  $f_1$  to increase and its amplitude to decrease. The increased  $f_1$  will help reduce fatiguing in the anode, since the energy inputs of the engine decrease at frequencies above 1000 Hz. The decreased amplitude has two beneficial effects: It insures against abrasion and it will reduce the number of large pulses caused by the vibrations. There is one detrimental effect in reducing the cathode length and that is a lower detector efficiency. However, since the diameter was increased (in the previous suggestion) it is felt that the same efficiency can be achieved. These recommendations, along with the previous suggestions, should yield a detector with a lifetime of 2000 hours or more.

Recommendations for Further Study. The previous two sub-sections have been concerned with modifying the present detector. However, because the basic materials used are not highly halogen inert, they can never be combined to yield the ultimate long-life detector. Although an unlimited lifetime is not considered feasible, lifetimes in excess of 6000 hours have been recorded by using materials totally inert to halogen attack (Ref 3:1202). Thus, it is felt that with further investigation, materials can be found and procedures formulated, that will yield a G-M tube capable of existing in the aircraft environment for periods exceeding 3000 hours.

It is the purpose of this section to forward recommendations for further investigation and experimentation in order that this truly long life G-M tube can be developed. In order to cover this topic

completely, these recommendations are divided into the four primary components of the G-M tube:

1. The cathode,
2. The anode,
3. The insulators, and
4. The sealants.

Suggestions for each area are made and then discussed in the same sequence.

The first item recommended for further study is the cathode. It appears that the most significant problems can be remedied by using materials totally resistant to halogen attack. However, there are other contributing factors that must be considered, of which efficiency and expansion coefficients are two. Some materials which indicate promise are:

1. Thin-walled Pt-Ir tubing contained within a stronger and more workable cylinder (e.g., glass or stainless steel),
2. E-C ( $\text{SnO}_2$ ) coated glass, and
3. Pure nickel or high nickel alloys.

These three recommendations are listed in order of preference. The platinum-iridium tube is inert to halogens and also yields the highest efficiency. However, construction problems are the largest drawbacks and must be investigated.

The E-C coated glass is also totally inert to halogen gas, but it is lower in efficiency than Pt-Ir. However, E-C coated glass is considerably more workable than Pt-Ir and possibly a larger cathode could be used to compensate for its efficiency.

Nickel is the least preferred, since little is known about it. Theoretical studies indicate that it is halogen resistant, and its efficiency is better than tested samples of E-C coated glass. However, its expansion coefficient is  $13 \times 10^{-6}/^\circ\text{C}$ , which is much greater than glass sealants or forsterite insulators ( $9.0 \times 10^{-6}/^\circ\text{C}$ ). It is hoped that the expansion coefficient problems will be solved, then materials such as Ni will offer additional possibilities.

The anode is the second component to be considered. With the anode, it is extremely important to match: Halogen resistance, vibrational strength, and expansion coefficients. Again a preferential list of possibilities is made and each will be discussed in the order presented:

1. Nickel-beryllium,
2. E-C ( $\text{SnO}_2$ ) coated glass wire, and
3. Small diameter (5 mil) Pt-Ir wire wound around a small glass cylinder.

The Ni-Be wire has outstanding strength and since it is composed of 98 percent Ni, it should be highly resistant to halogen attack, however this must be verified. The primary objection to this material, is the same as for a Ni cathode [i.e., its expansion coefficient is high ( $14 \times 10^{-6}/^{\circ}\text{C}$ )].

As stated before, the E-C coated glass is highly resistant to halogen attack, but little is known of its vibrational characteristics. Before this material could be recommended for use, these vibrational characteristics must be determined. Another factor (which may or may not be a problem) is that the minimum diameter this wire can be drawn to, is  $\sim 40$  mils and thus some increase in  $V_s$ , may be noted.

The last suggested anode is the use of a glass rod wrapped with Pt-Ir wire. The advantage is the combination of truly halogen resistant and vibration resistant materials. There are some unknowns though, such as: How is the efficiency and operation of the detector affected by this anode configuration and will the glass cylinder actually withstand aircraft vibrations. Again this suggestion cannot be utilized until these questions are answered.

Although there are several other materials available for use as cathodes and anodes, it is felt that those presented show the most promise. Considerable effort is required, however, to prove their utility.

The third area of recommended study deals with insulators. Here unfortunately, there is little from which to choose. As a matter of fact, the only choice readily available is glass. Actually, this recommendation calls for the entire counter to be made from glass, utilizing an internal cathode constructed of Pt-Ir, Ni, or E-C coatings. One step in the problem of matching expansion coefficients can be avoided by eliminating the forsterite insulators. However, this requires a study of new designs, and then their construction and testing prior to drawing any firm conclusions. Even though this is fairly complex, it does offer some very good possibilities and further investigations should be made.

The last area recommended for further study is detector sealants. The purpose of these sealants is to "seal" the gaps between all the different counter materials. Thus, one of its primary factors is to have an expansion coefficient comparable to metals. Up to the present, the only available materials were glass solders. However, in order to give glass the required high expansion coefficient, it must have a high lead content. As shown by the surface analyses, the lead results in bromine attack; therefore, it is strongly recommended that this form of sealing be replaced. One strong candidate for this purpose is epoxy. Epo-Tek Incorporated (Ref 8:) manufactures a wide variety of epoxies capable of sealing at low pressures ( $10^{-7}$  torr) and high temperatures ( $190^{\circ}\text{C}$ ) and not outgas appreciably. The sheer strength, glass-to-metal adhesiveness, and sealing ability of epoxy add to its attractiveness as a basic component of G-M tubes. The only unknown characteristic of epoxy is its halogen resistance, and this will have to be determined prior to being given any serious consideration. However, if epoxy

is halogen resistant, it eliminates the expansion coefficient problems and "opens-the-door" to a wide variety of materials. Because of its strength and versatility, it has a wide range of possible uses, such as:

1. Supports for the anode wire,
2. Insulators (non-conductive epoxy),
3. Electrical contacts (conductive epoxy), and
4. General sealants.

With these suggested areas of study, the final segments of this thesis are brought to a close. Even though the ultimate design for the perfect G-M tube has not yet been found, the foundation and framework for future efforts has been assembled. The study and testing that remain, although extensive, will almost assuredly result in the final product: A truly long-life "rugged" G-M tube.

## Bibliography

1. Ahearn, A.J., Mass Spectrometric Analysis of Solids. New York: Elsevier Publishing Company 1966.
2. Cabot Corporation. (Stellite Division). "Corrosion Resistance of Hastelloy Alloys". Cabot Corporation (Stellite Division) Brochure: 2-63
3. Clark, L. B. Sr. "G-M Counters for High Temperature Operations". The Review of Scientific Instruments, 26:1202 (1955).
4. Couch, R. P. and J. Clark. Technical report on vibration testing to be published by the USAF Flight Dynamics Laboratory, at a later date (1972).
5. Curran, S. C. and J. D. Craggs. Counting Tubes. New York: Academic Press Incorporated (1949)
6. Diethorn, W. "Methane Proportional Counter System for Natural Radiocarbon Measurements". NYO, 6628 (16 March 1956).
7. Dooley, G. J. III and T. W. Haas. "Auger Electron Spectroscopy: Metallurgical Applications". USAF Aerospace Research Laboratory 70-0337: 1-8 (1970).
8. Epoxy Technology Incorporation. Private communications in December 1971.
9. Gisclard, B. Technical report on halogen detection by use of methyl orange reagent to be published by USAF Flight Dynamics Laboratory at a later date (January 1972).
10. Hamilton Watch Company. Brochure on Elinvar Extra from Precision Metals Division, Lancaster, Pennsylvania 17604.
11. Hodgman, D. D. (Editor). Chemistry and Physics Handbook (Fourtieth Edition). Cleveland: Chemical Rubber Publishing Company, 1959.
12. International Nickel Company. Private communications (December 1971).
13. Kandrach, G. Private communications with Corning Glass Works in November 1971.
14. Kiser, R. W. "Characteristic Parameters of Gas-Tube Proportional Counters". Applied Scientific Research, B 8:183 (1960).
15. Korff, S. A. Electron and Nuclear Counters (second edition). New York: D. VanNostrand Company, 1955.
16. -----, Geiger Counters Theory, Operation, and Manufacture (Ad 708 922). New York: National Technical Service, 1970.
17. Lampe, F. W., J. L. Franklin, and F. H. Field. "Cross Sections for Ionization by Electrons". Journal of the American Chemical Society, 79: 6129 (1957).
18. Layne, A. A. (Editor) "Materials Engineering 1971 Material Selector". Reinhold Publishing Corporation, November 1970

19. Liebson, S. H. and H. Friedman. "Self-Quenching Halogen Filled Countdrs". The Review of Scientific Instruments, 19: 303 (1948).
20. Mahoney, J. J. "Specifications for Ruggedized Radiation Detector Assembly". General Nucleonics Division/TYCO ES-902-01: 5-6 (1971).
21. ———. "Acceptance Test Procedure for Radiation Detectors". General Nucleonics Division/TYCO at 1000-1A-05: 12 and 13 (1971).
22. Mitrofanov, N. "Method of Increasing the Maximum Operating Temperature of a Radiation Detection Device". U.S. Patent Office 3, 342, 538: 1-12 (1967).
23. Pannhacker, R. G. and R. W. Kiser. "Characteristic Parameters of Geiger-Muller Counter Gases". Applied Scientific Research, B10: 41 (1962).
24. Parr, J. G. and A. Hanson. "An Introduction to Stainless Steels." Metals Park: American Society for Metals, (1965).
25. Price, W. J. Nuclear Radiation Detector (second edition). New York: McGraw-Hill Book Company, 1964.
26. Rossi, B.B. and H.H. Staub. Ionization Chambers and Counters. New York: McGraw-Hill Book Company (1949).
27. Solomon, J.S. and W.L. Baun. "Content Mapping Techniques for Qualitative and Semiquantitative Analysis with the Electron Microbeam Probe". Air Force Materials Laboratory Technical Report 70-146: 1-19 (1970).
28. Storrs, C. D. and R. W. Kiser. "Characteristic Parameters of Geiger-Muller Counter Gases". Applied Scientific Research B8: 387 (1960).
29. Uhlig, H. H. The Corrosion Handbook. New York: John Wiley & Sons Incorporated, 1948.
30. Usacev, S. and M. Seman. "Threshold Oscillations in Bromine Quench G-M Counters". Nuclear Instruments and Methods 73: 41-44 (1969).
31. ———. "Supplemental Work on the Optimum Cathode Thickness of G-M Counters for Gamma Radiation". Atomkernenergie 4: 135-8 (1959).
32. Ward, A. L. and A. D. Krumbein. "Some Characteristics of Chlorine Quenched Geiger-Muller Counters". The Review of Scientific Instruments 26 No 4: 341 (1955).
33. Wilkinson, D. H. Ionization Chambers and Counters. Cambridge: Cambridge University Press 1950.



## Appendix A

### Theory of G-M Counter Operation

The theory of radiation counters has been studied extensively. Rose, Korff, Present, Liebson, Curran, Craggs, Friedman, Loeb, and a number of others are responsible for the development of the fundamental theory, and their works are used, in part, for this paper.

The Geiger-Muller counter is one form of a gas filled radiation detector (ionization chambers and proportional counters are others) used to detect and count ionizing events caused by incident  $\alpha$ ,  $\beta$ ,  $\gamma$ , and/or x-radiation. These counts then give a relative measure of the radiation field strength in the vicinity of the detector. Of particular interest in this study are the particles from  $Kr^{85}$  [ $\beta \sim 0.67$  MeV, (maximum),  $\gamma = 0.54$  MeV] and  $Cs^{137}$  [ $\beta \sim 0.52$  MeV (maximum),  $\gamma = 0.66$  MeV] since  $Kr^{85}$  is the source used on USAF aircraft oil-quantity indicating systems and  $Cs^{137}$  is the source used in most of the experiments described in this thesis.

Although G-M tubes can be made in a variety of geometrical shapes and sizes, the most common design is that of two concentric cylinders. The inner cylinder is called the anode and is maintained at a positive potential with respect to the outer cylinder or cathode. The space between the anode and cathode is filled with gas or gas mixture. The pressure within the tube may vary, depending upon the use for which the tube is designed: e.g., on USAF aircraft, the mixture is composed of neon-argon and halogen gas at an internal pressure of 350-400 torr.

In order to detect incident radiation, two major components are required: A counter and an electronic sensing circuit. Fig. 2 (page 11) represents a fundamental circuit composed of H.V. source, sensing resistance, capacitance, and counter (also a load resistor which is optional).

G-M counters may be either self-quenched, wherein plasma and/or passive gaseous phenomena are used to extinguish the discharge, or externally quenched. Although the use of external circuitry is a fairly efficient means of quenching, it is not presently used on USAF aircraft and thus will not be a major subject of this report. In explaining the electronics, it is sufficient to note that the circuit rapidly lowers the voltage to below starting voltage immediately after an ionizing event occurs and then increases the potential back to the original level until another event takes place.

The self-quenching G-M counters generally use either polyatomic vapors or diatomic (halogen) gases, as quenching agents. The main disadvantage of a polyatomic molecule is that during the quenching action it dissociates into atoms that rarely recombine into the same molecule. Even though the polyatomic molecule can dissociate into further discharge quenching vapors, it eventually depletes itself causing the tube to go into continuous discharge. On the other hand, the halogen molecule disso-

ciates into two atoms upon its neutralization at the cathode. Since these atoms will eventually recombine, the halogen gas is never depleted. This is true, however, only if the dissociated molecule does not react with the surfaces of the chamber. The fact that the dissociated species are highly reactive, presents a serious problem and the counter materials must be chosen with extreme caution for this reason.

It should be noted that no radiation can be detected unless an electron is formed within the sensitive volume of the chamber. There are three ways in which electrons may be formed within the counter:

1. By direct photoelectric interaction in the gas or the photo effect in the cathode wall, and subsequent migration of the photo electron into the sensitive volume.
2. By the Compton effect in the gas or cathode wall and then the subsequent migration of the Compton electron into the sensitive volume.
3. By pair production and the subsequent migration of the electron into the sensitive volume.

Each of the processes is a function of the photon ( $\gamma$  ray) energy, fill gas, wall thickness, and wall material, and the probability of such a process occurring is generally much less than unity. As a result, the efficiency of most G-M counters in detecting radiation is small (Ref 15:187).

In the remaining two phenomenon, the probability of electron production is much more likely in the cathode wall than in the gas simply because of density and collision cross section considerations. Compton effect and/ or photoelectric effect in the wall are both dependent upon photon energy and the wall material i.e., for a given photon energy, the ratio of photoelectric to Compton events will vary for different materials. For example, the electrons produced by a 0.6 MeV photon in Cu ( $Z=29$ ) will be by 98 percent Compton and only 2 percent photoelectric. Whereas electrons produced from Pb ( $Z=82$ ) by the same photon will be by 58 percent Compton and 42 percent photoelectric. Hence, there is a definite dependence upon atomic number (see "The Efficiency Experiment" section for detailed discussion).

Once an electron has been formed within or has migrated into the chamber, the electron is subjected to the electric field between the two concentric cylinders. This field varies according to the following relation:

$$E = \frac{V}{r \ln \frac{r_b}{r_a}} \quad (7)$$

where  $r_b$  radius of cathode and  $r_a$  radius of anode such that  $r_a < r_b$ ,  $V$  is the applied voltage. This means that the electron will drift toward the anode wire and its kinetic energy will increase between successive collisions. If  $V$  is equal to or greater than the threshold or starting potential ( $V_s$ ) of the counter, then the electron will eventually possess sufficient kinetic energy to produce ion-pairs upon collision with neutral gas molecules. The negative ion will travel toward the cathode. The electrons thus produced, also drift.

toward the anode in the  $\vec{E}$ -field, creating additional ion-pairs. The process continues and eventually results in a cascade or Townsend avalanche.

The avalanche begins approximately 5 wire radii (Ref 33:170) out from the cylinder axis and then spreads pyramidally towards the anode wire. The base of this pyramidal form is located along the anode and is approximately 0.04 cm long (Ref 33:170). The discharge then travels down the anode wire by successive avalanches. The means by which additional avalanches are formed was for a time unexplained, however, the primary process has generally been considered to be that of cumulative excitation coupled with photon transport. When the initial avalanche occurs, species excited in the process emit photons within a wide energy range, and although this radiation is not of sufficient intensity to ionize another atom or molecule of the same species, it could ionize a species of lower ionization potential. Halogen quenched G-M tubes contain neon, argon and chlorine or bromine. According to A.L. Ward and A. D. Krumbein (Ref 32:315), the halogens do not appreciably absorb the photons responsible for the discharge spread. This then leaves only argon. However, the percentage of argon is so very small ( $\sim 0.1$  percent) that it is unlikely to be responsible for the discharge spread. Therefore, it appears that a stepwise collisional excitation, coupled with absorption in the neon carrying gas is the most likely means by which the discharge spreads along the anode wire.

Each successive avalanche probably overlaps its predecessor somewhat, but the overall discharge is carried further down the anode wire until the entire length has been covered. The velocity of the spread has been measured by several observers and all seem to agree that the velocity is approximately  $10^7$  cm/sec (Ref 33:192, Ref 15:179).

It should be noted that if the initial avalanche is formed at some point other than one end of the wire, then the discharge will progress in both directions at the same velocity until the entire wire is covered.

As the discharge forms and traverses the anode length, the electrons are collected on the anode leaving a positive-ion sheath formed around the anode wire. The movement of this sheath is essential to the discussion of the counter operation. As the sheath forms, it reduces the electric field in the vicinity of the anode. This reduction is sufficient to prevent any further ionizing event within it and thus momentarily quenches the discharge. Because the sheath is composed of positive ions, it will travel radially outward to be collected on the cathode. As it travels, the field between it and the wire will increase until such time as another ionizing event can take place and be detected. This elapsed time is known as the dead-time and corresponds to the distance the sheath has moved (in the dead-time), called the critical radius ( $r_c$ ).

Even though the formation of the positive-ion sheath momentarily quenches the discharge, there are still many highly energetic species present within the counter which could re-initiate the ionizing process and thus give spurious counts. Because of this, these energetic species must be quenched. This is accomplished in two ways: internally and externally.

Internally the discharge is quenched by two mechanisms, the formation and movement of the positive-ion-sheath, as discussed above, and by the interactions of the gas within the tube. During the discharge, the metastable states of neon are readily excited and if allowed to exist in this state, would eventually radiate enough energy to re-initiate the discharge. However, since argon, bromine, and chlorine all have ionization potentials lower than the neon metastable state energy, a collision between a neon metastable atom and argon, bromine or chlorine molecule, would in effect, neutralize the metastable state of the neon molecule.

The collision between a neon metastable atom and an argon neutral molecule will produce an argon ion which will then proceed toward the cathode. The collision between the neon metastable atom and the halogen molecule will neutralize the metastable atom and ionize the halogen molecule. In turn, the ionized halogen molecule will proceed out to the cathode where it will be neutralized by absorbing an electron from the wall. The argon ions that are formed by the collision with neon metastables will collide with the halogen molecules and ionize them. The argon ion will be neutralized into an argon molecule and the ionized halogen atom molecule will be neutralized at the cathode.

Upon neutralization, the halogen molecule will dissociate into two highly energetic atoms that will eventually recombine to form a neutral halogen molecule if there is no interim reaction with counter surfaces. Because of the reactivity of most materials with halogen gases, the common cathode metals cannot be used without surface protection. The materials most used in halogen counters are stainless steel, tantalum, and treated glass. One method of giving these surfaces added resistance to attack is passivation which entails elevating the temperature of the counter with the halogen gas inside. This process builds up a halide layer on the surface, consequently reducing its reactivity. Although passivation "works", any action which would cause the layer to "flake-off" or rearrange its crystalline lattice could then expose the unpassivated surfaces below and a halogen reaction would again take place. Another method of protecting the surface involves electroplating or sputtering with non-reactive metals such as platinum or platinum-iridium. Although Pt-Ir is very halogen resistant, even at elevated temperatures, plating/sputtering is difficult and quite expensive. In addition, platings/sputterings are exceedingly hard to put on smoothly and almost impossible to keep from forming small pinholes in the surface. Further, these preparations require considerable time. It would appear that the use of non-reactive surfaces for the entire counter would be the most logical solution and this is one of the main areas of this study.

Other complications which enter into the problem include the efficiency of the cathode material and its ability to withstand high temperatures and vibrations.

Externally, the discharge can be extinguished by using the aforementioned quenching circuit. But since this is not employed on USAF aircraft, it will not be covered here. However, the impedance of the sensing circuit is directly related to the quenching ability of the counter. A simple experiment was performed in which a counter was operated in a circuit with "zero" impedance. The result was that the counter began operating normally at  $V_s$  and the internal quenching ability was sufficient to quench the discharge up to a certain voltage [critical voltage ( $V_c$ )]. Once  $V_c$  was reached, two distinct pulse shapes were detected: A small pulse, which was the typical pulse noted below  $V_c$ , and a much larger pulse which was detected upon reaching  $V_c$ . The small pulses signified the discharges quenched by the internal mechanisms and the large pulses were found to be quenched by the internal mechanisms and the large pulses were found to be quenched by a combination of circuit impedance and internal mechanisms. In the low impedance circuit at  $V_c + \sim 10$  volts, the counter would go into continuous discharge. It was found that by increasing the circuit impedance, a greater amount of voltage could be applied prior to going into continuous discharge. This gave the counter a longer operating voltage span, or plateau. With this in mind, an additional resistance [load resistor ( $R_L$ )] was placed in series immediately behind the counter. The load resistance increases the circuit impedance and thus the operating range of the counter. Another simple experiment was performed to determine the optimum position for  $R_L$ . It was found that the advantageous effect of  $R_L$  was decreased as it was moved further from the G-M tube. Therefore, for the maximum beneficial results, the load resistance should be as close as possible to the counter. Another result of this experiment indicated that the size of  $R_L$  is not as important as its presence or its position. Thus a resistance of  $1.0 \text{ M}\Omega$  would have the same basic effect as a  $5.0 \text{ M}\Omega$ . It was also noted that  $R_L$  would increase the count-rate, for any given counter, at least for the initial portion of the plateau.

If an oscilloscope were used to depict the pulse pattern observed from a G-M tube through a sensing circuit, it might look like Fig. 19. As the counter breaks down into discharge, it produces the fast rise in the pulse. This is due to the ionization within the chamber and the collection of the charge (electrons) on the anode. The pulse height then tapers off and returns to zero volts as a function of the RC time constant of the sensing circuit. Each pulse thus formed constitutes a count. It is significant to discuss the decaying portion of the pulse, since the speed with which the tube returns to normal is a measure of the speed at which the tube can count. To do this, two definitions are needed: The dead time and the recovery time. The dead time was stated earlier as the time it takes for a counter

to recover to the point at which another pulse could be detected and the recovery time is the time elapsed between initial pulse and the next pulse of full amplitude.

These definitions are easier to understand by the use of Fig. 19. As can be seen, the first pulse is indicative of the tube as it operates from a normal condition, discharges, and then returns to normal. After the first pulse and before the tube can return to normal, a second small pulse can be detected. This corresponds to another ionizing event, but since the tube has not returned to normal, the field in the vicinity of the wire is lower and thus, the small pulse. As the tube continues to return to normal operating voltage, the pulses grow until finally another pulse is detected that has the same height as the first pulse. The time between the first and second pulses in Fig. 19 is the "dead-time". The time between the first and the last pulse is the "recovery-time".

An alternate way of describing these events is by the movement of the positive ion sheath. The movement of the sheath was discussed before but its relation to the detected pulse was not stressed. When the discharge takes place and the electrons are collected on the wire, a positive ion sheath surrounds the wire. Because of its closeness to the wire, the electric field is reduced to the point where no avalanche can be initiated and thus, no discharge can occur. As this sheath begins to move radially outward toward the cathode, the electric field around the wire increases. When the sheath has progressed far enough so that an avalanche could form, then a small pulse could be detected. This distance that the sheath has moved was referred to earlier as the critical radius and the time from the first pulse until  $r_c$  is reached was noted as the dead-time. As the sheath continues to move outward, the field continues to increase and the detected pulses also grow in height for each successive ionizing event. Once the sheath has traveled to the cathode wall and has been neutralized, the pulse will have returned

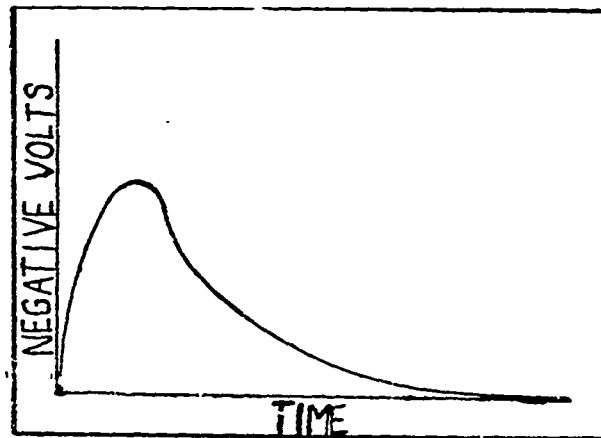


Fig. 18. Oscilloscope Displayed Geiger Pulse

TIME  
Fig. 19. Dead Time and Recovery Time(Ref 5:68)

to its maximum amplitude (see Fig. 19). The time lapse between the first pulse and neutralization of the ion sheath at the cathode is called the recovery time of the counter. In the counters under present investigation, the dead times are  $\sim 80-90 \mu\text{sec}$  and the recovery times are  $100-300 \mu\text{sec}$ . This compares favorably with literature (Ref 15:133). Although these times can vary depending upon the gases used within the counter and the applied voltage. In general, the heavier the gas, the greater the dead and recovery times. This, in turn, corresponds to the mobility of the ions of the respective gases.

The last portion of the theory is concerned with the dependence of  $V_s$  on the counter variable. The factors that most effect the starting voltage of G-M tubes are; total pressure within the counter, percent of halogen gas (halogen quenched tubes), the radius of the anode ( $r_a$ ) and the radius of the cathode ( $r_b$ ). The inter-relationships of these factors can be quite intricate and depend significantly on whether a halogen or polyatomic gas is being used as the quencher. The total pressure within the counter has the same effect regardless of the type of gases used i.e., increasing pressure yields an increase in  $V_s$ . This is a nearly linear relationship which has been experimentally plotted by several observers (Ref 33:179, Ref 19:306).

While both the anode and cathode radii effect  $V_s$ , the anode radius is by far the dominant factor. However, when dealing with halogen counters, radii from 5 mil to 40 mil have negligible effect on  $V_s$  (Ref 19:304). The reason for this appears to be in the lower ionization cross section in halogen counters as opposed to organically filled counters. Also, the mean free path in halogen counters is longer by a factor of 100 (Ref 16:49). Thus the electron will gain sufficient energy to ionize at appreciable distances from the anode. Since there is no point in making the wire diameter less than one free path length, a larger anode may be used.

The last variable that must be considered is the percentage of halogen gas in the mixture. The effect of varying the percentage of halogen gas was first studied by Liebson and Friedman (Ref 19:304). From their work, the aging characteristics of halogen counters can be deduced. In essence, the result of the dissociated atoms of halogen molecules reacting with the internal counter surfaces causes a reduction in halogen content within the chamber. This reduction was found to be accompanied by a drop in  $V_s$ . Although there would also be a reduction in overall counter pressure, the halogen gas composes only about 5 torr in a 3 cubic centimeter tube, whose overall pressure is 350 torr. A loss or gain in this small amount would be negligible unless there is a much stronger relationship. Graphs of  $V_s$  versus halogen content can be found in the works of Ward and Krumbein (Ref 32:349), and Liebson and Friedman (Ref 19:304).

A relationship exists between halogen gases and argon which is very important when attempting

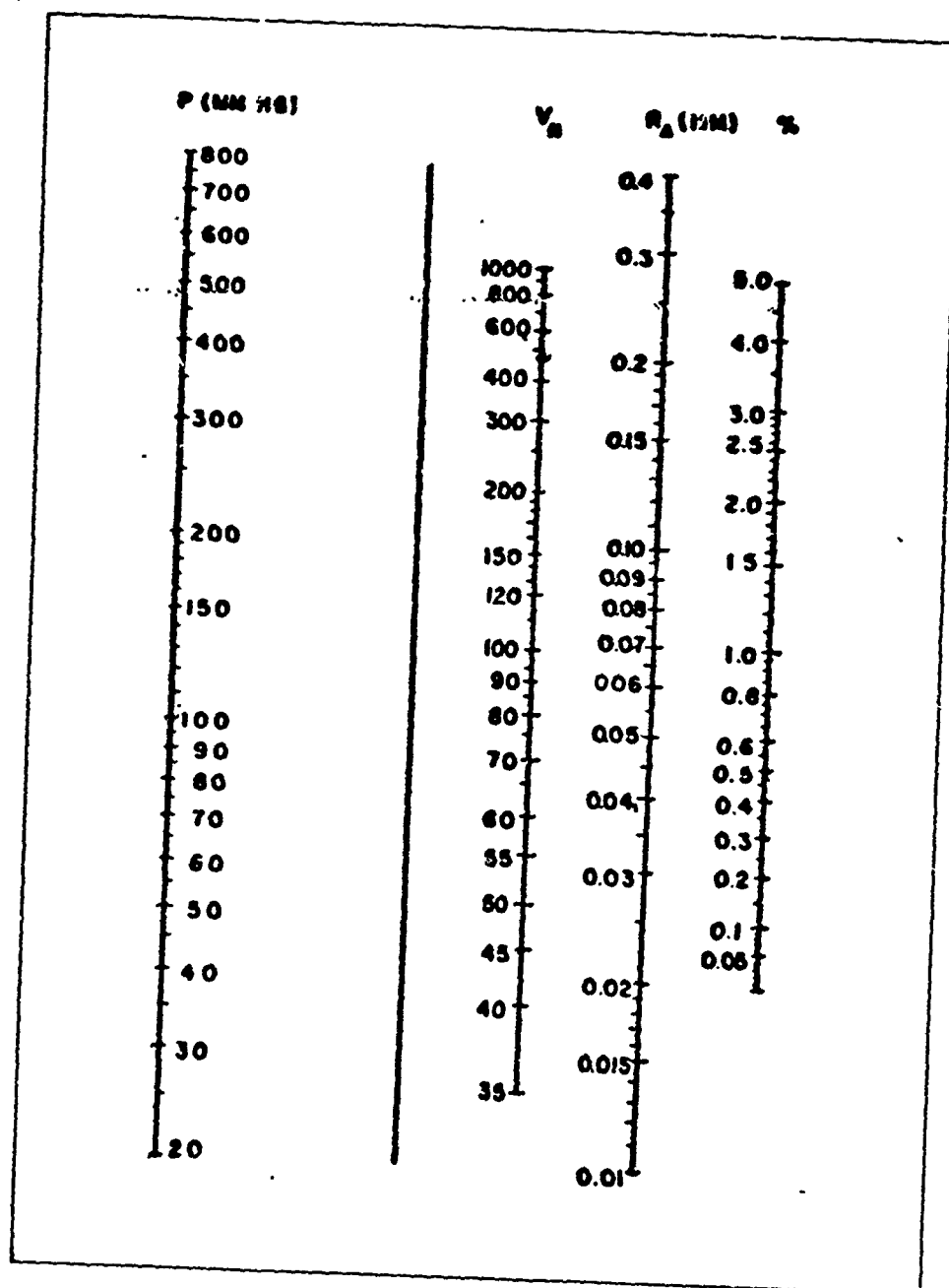


Fig. 20. Nomograph for obtaining normalized starting potential ( $V_n$ ) for a neon-chlorine counter. To obtain  $V_n$  for given values of total pressure, anode radius and chlorine percentage, a straight line is first drawn between the desired pressure ( $p$ ) and the wire radius ( $r_a$ ). From the intersection of this line with the unmarked vertical line, a straight line is drawn to the chlorine percentage line. The intersection of this last line and the  $V_n$  column gives the normalized starting potential (Ref 32:344).



to adjust  $V_s$ . We have seen that with the overall chamber pressure held constant and increasing the halogen content will result in an increased  $V_s$  (and vice-versa). However, if the overall pressure is held constant and the argon content is increased, no variation in  $V_s$  is noted, but an increased ability to quench the metastable states of neon has been gained. Therefore, maintaining a constant overall pressure and increasing the argon content while decreasing the halogen content will result in a lower operating potential for the counter. However, at very low halogen content, continuous oscillations have been observed. Since these have been described as critical metastable state quenching/non-quenching phenomena (Ref 28:41), it is essential to proper counter operation to have very precise measurements of the gaseous mixture.

Many authors have attempted to predict  $V_s$  for a given counter without resorting to experiments. At best, this has met with limited success. Probably the greatest success was attained by Ward and Krumbein (Ref 32:344). By proving that the Lanterjung equation:

$$\log \frac{E_s}{P} = \frac{b}{V_n} + \log(a + d\%) \quad (8)$$

where  $V_n$  = normalized starting potential

$$V_n = \frac{V_s}{\ln \frac{r_b}{r_a}} \quad (9)$$

and where a, b, and d, are constants (% = amount of organic quench gas) held not only for organically quenched counters, but also for halogen counters, they were able to construct the nomograph in Fig. 20. This relates the  $V_s$  to overall pressure, percentage of chlorine and the radius of the anode. This can be expanded to apply to a variety of anode radii (40mils without any real loss in effectiveness since  $V_s$  is not strongly dependent upon  $r_a$ ).

Another factor that has been used to interrelate the various counter variables is the gas multiplication ( $A_0$ ). This is defined as the average number of electrons reaching the anode per electron liberated in the initial ionizing event. Originally, it was postulated by Rossi and Staub (Ref 26:73, 74, and 77) that any equation that related the gas multiplication factor to the counter variables, had to satisfy the condition

$$A_0 = f\left(p r_a, \frac{V_0}{\ln \frac{r_b}{r_a}}\right) \quad (10)$$

where p is the tube pressure,  $V_B$  = applied voltage,  $r_a$  and  $r_b$  are the anode and cathode radii respectively. After many revisions Diethorn (Ref 6:6628) derived the most successful relationship, which is:

$$\ln A_0 = \frac{V_0 \ln 2}{\Delta V \ln \frac{r_b}{r_a}} \ln \left[ \frac{V_0}{K \rho r_a \ln \frac{r_b}{r_a}} \right] \quad (11)$$

In this formula, two new constants are introduced:  $\Delta V$  and  $K$ .  $\Delta V$  is the potential difference through which an electron drops between successive ionizing events. The electrons that are being referred to here, are the ones that are ejected into the sensitive volume either by the photoelectric effect or Compton effect in the cathode wall.  $K$  is the value of the reduced electric field where multiplication begins ( $K = \frac{E_0}{p}$ ). In other words, for a given counter and gas at some constant pressure there exists a critical value for the electrical field ( $E_0$ ) below which ionizing events cannot occur. This equation solved many of the problems that were present in theory prior to Diethorn, but along with this solution came the complication of determining  $\Delta V$  and  $K$  for a particular counter and gas mixture. Although a total solution has never been found, much work has been performed by R. W. Kiser and associates (Ref 23:41-48; Ref 28: 387-396). Dr. Kiser (Ref 14:198) found that these two constants were related to the ionization cross-section of 75 volt electrons by the following equation:

$${}_{75}\sigma_i = 8.1 \times 10^{-17} \frac{K}{\Delta V} \quad (12)$$

Several values of the cross-section of 75 volt electrons are contained in Ref 17:6130, but  $K$  and  $\Delta V$  remain essentially unknown.

Dr. Kiser also found that  $\Delta V$  was related to the energy necessary to create an ion pair ( $W$ ) in a given mixture and also to the percentage of discharge propagation due to Townsend avalanches (%T). This is expressed as:

$$\%T = 100 A_0^{(\frac{\Delta V}{W} - 1)} \quad (13)$$

In the G-M region around  $V_0$ ,  $A_0 \sim 10^7$ . Thus, if the percentage of propagation due to Townsend avalanche can be expressed, the solutions for  $\Delta V$  and  $K$  can be gained.

In the preponderance of literature, the percentage of the propagation in the G-M region, is attributed almost solely to photons, and a low value ( $\sim 0.1$ -10 percent) can safely be assumed for %T. The reason that %T is so low is because all that is needed is one successful Townsend avalanche and then the photons radiated by the excited species within the avalanche will be sufficient to continue the discharge.

There are many "loose ends" in this approach that make it of questionable value. First of all,

the average energy to create an ion pair in a mixture is assumed to be a weighted addition of the parts that compose the mixture. Although this is not strictly correct, it can admittedly be used as a rough approximation. Secondly, the %T is not known definitely and therefore must be assumed. Finally,  $75\sigma_i$  has not been measured for all desired gases. Although this does not make the theory incorrect, it does make it less useful.

Once all the constants are found, the gas multiplication factor can be determined; however,  $A_0=10^7$  has already been assumed in the G-M region, therefore the end result is again of less than significant value. But, by assuming  $A_0=10^7$  it is possible to determine a  $V_s$  for a G-M counter. Rearrangement of Equation 11 yields the following form:

$$\frac{\Delta V (\ln A_0) (\ln \frac{r_b}{r_a})}{\ln 2} = V_s \left[ \ln V_s - \ln K p r_a \ln \frac{r_b}{r_a} \right] \quad (14)$$

Although it has not been done in this paper, it is possible to get a series of values for  $V_s$ , by inputting different values of  $\Delta V$  and  $K$  into a computer program. Again, it should be stated, that this conclusion is built upon assumed values and from this standpoint is of questionable value.

This completes the background theory of the operation of Geiger-Muller counters. It is hoped that this has provided a basic understanding of the operations and processes that take place within a counter. It may be worthy to note at this point that, although the Geiger-Muller tube is one of the oldest, simplest, and most frequently used counters, the detailed molecular and plasma processes which occur inside are not (even yet) totally understood.

The Composition, Halogen-Resistance, and Vibrational  
Characteristics of Various Materials

This appendix gives some general information on several metals that either have been used as materials in halogen G-M tubes or those that appear as likely prospects. An alphabetical listing of the materials, some basic characteristics, uses, and halogen reactance is followed by a chart showing the materials vibrational characteristics.

There is little information on ceramics, glasses or epoxies since no real data was found to indicate their resistance (or lack thereof) to halogen gases. However, from private communications with Corning Glass Works and Epo-Tek (Refs 13, 8) the glasses and epoxies appear to have good resistance to halogen attack. An investigation is under progress at USAF Flight Dynamics Laboratory to actually determine the reactivity of several types of epoxies and sealing glasses. This study is being conducted by 1/Lt. L. Tessler and supervised by Capt. R. P. Couch.

Beryllium

Beryllium is a high strength but low density material. It is widely found but only in small quantities. Its primary drawback is its expense, but a small addition of beryllium to other metals yields an alloy of much greater endurance (Ref 11:408)

In its pure state, beryllium is attacked by fluorine at room temperature and by chlorine, bromine, and iodine at "elevated" temperatures (Ref 29:56). A private communication with Little Falls Alloy, Inc. revealed that "elevated" temperatures was probably at approximately 100-150°C.

Hastelloys

Hastelloys A, B, and C are all high Ni (61-82 percent) Mo (16-28 percent) alloys. Each of these are quite hard (especially "C") and are extremely difficult to machine. Of all Hastelloys the "C-276" alloy is most workable.

Hastelloys are very good in halogens and have maximum recommended temperatures in dry chlorine of 500°C. When resistance to corrosion is desired, both at high temperatures and below the dew point, the order of preference is Hastelloy B, A and then C (Ref 29:861-862). However, the "Stellite Hastelloy Corrosion Guide" (Ref 2:13-17) indicates that, in dry Br<sub>2</sub> or Cl<sub>2</sub>, Hastelloy C is the most desirable, with less than 2 mil penetration per year for Cl<sub>2</sub> at 300°F and 20 mil per year for Br<sub>2</sub> at 150-700°F.

Molybdenum

Molybdenum does not occur in nature, but must be obtained from "molybdenite" (MoS<sub>2</sub>) and/or from "wulfenite" (PbMoO<sub>4</sub>). It is extremely hard and is used to increase the toughness and tensile

strength of steels. It is softer than tungsten and its ductility makes it extremely useful as filaments grids and screens in radios (Ref 11:421).

Molybdenum is not resistive to halogen attack at all. It reacts with fluorine at room temperature and with chlorine and bromine at red heat (Ref 29:252).

### Nickel

Nickel is a hard but malleable metal which is slightly magnetic. It has been used extensively in alloying with other metals to increase their strength and corrosion resistance.

Gases such as chlorine, bromine and other halogens are appreciably corrosive to Ni only when they contain condensed moisture (Ref 29:265). As a matter of fact, at 315°C and in dry chlorine nickel is superior to Inconel, Monel or any of the Hastelloys (Ref 29:682).

### Nickel Iron Alloys (Elinvar Extra)

"Elinvar Extra" is a precipitation hardening Fe-Ni alloy having a constant elastic modulus and "zero" thermoelastic coefficient over a temperature range of -50° to +150°F. It is vacuum melted to assure maximum uniformity of composition and internal cleanliness" (Ref 10:1-2 ).

Although no definite information has been found on the halogen resistance of Elinvar, Ni (and some high Ni alloys) provide useful resistance to chlorine over a wide range of concentration and temperature (Ref 29:681). Because of its Ni content, Elinvar Extra is considered by its manufacturer (Ref 12) to be very good in halogen environment.

### Platinum Alloys

Platinum usually occurs in native form, accompanied by small quantities of iridium, rhodium and osmium, all in the same group. Pt is a tin-white metal of metallic luster, tenacious, malleable and ductile. The metal is not oxidized by air at any temperature, but is corroded by halogens, cyanide, sulfur and caustic alkalies (Ref 11:424).

All the free halogens react with Pt over certain ranges of elevated temperatures, but the addition of iridium or ruthenium increases Pt's halogen resistance. Of all the halogens Br<sub>2</sub> (dry) attacks Pt the most. Pt-Ir alloys are particularly suitable for use in halogen environments (Ref 29:300-310).

### Stainless Steels

446 stainless steel is best in corrosion resistance of the common commercial series, due to the high chromium content. It is quite sensitive to fracture at slight defects or notches, thus, commercial fabrication operations such as: drawing, spinning, forming, and welding require special care and precautions. Sigma phase may develop during service at elevated temperatures giving rise to increased

brittleness (Ref 24:50).

No definite information was found on the resistance of stainless steels to halogen attack with the exception of Unig's statement (Ref 29:145) noting that "In the presence of halogen ions, especially chlorine, the material must be looked on with suspicion". However, from surface analysis conducted as part of this thesis, both 17-7 Ph and 446 are attacked and considered to be non-effective in a bromine environment at 200°C.

### Tantalum

Tantalum is principally found in the mineral "tantálite". It can be drawn into a wire and has found use as a filament in lamps and as materials in halogen Geiger-Müller counters. It has been replaced in lamps by tungsten but still finds usage where "more than ordinary vibration" is possible (Ref 11:431).

At temperatures below 150°C tantalum is resistant to wet or dry chlorine. The same can be said of bromine with the upper limit of 175°C.

### Titanium

Titanium is a very malleable metal (hot or cold) unless contaminated with oxygen or nitrogen, however the smallest traces of these impurities embrittle the metal.

In its pure form, titanium's corrosion resistance is very similar to 18-8 stainless steel. It reacts with fluorine, chlorine and iodine at "elevated" temperatures.

### Tungsten

Tungsten is a hard, brittle, nonmagnetic metal and forms an oxide when heated in air. It has the highest known melting point of metals and thus its vapor pressure is very low. This makes tungsten useful for wiring furnaces, targets for x-ray tubes, and contacts. It has found its widest use as filaments in light bulbs and alloyed in steel to produce strong durable metals [e.g., armor plate and projectiles (Ref 11:433)].

All halogen gases react with tungsten, but at different temperatures. Bromine and iodine react with it at red heat and chlorine (in the presence of oxygen) reacts at 600°C (Ref 29:330).

Table IV  
Counter Materials, Compositions, and Vibrational Characteristics

Materials	Composition (%)	UTS= 10 <sup>5</sup> lbs./in <sup>2</sup>	Density lbs./in <sup>3</sup>	COE $\frac{10^{-6}}{^{\circ}\text{C}}$	Stress $\frac{10^3 \text{ lbs.}}{\text{in}^2}$	Length (in)	Vibrational Characteristics	
							f <sub>1</sub> calc Hz	f <sub>1</sub> Actual Hz
Elinvar Extra	43Ni, 5Cr, 3Ti, 48Fe	1.85	.294	8.1	58.4	2.38	1850	2221
Hastelloy C 276	56Ni, 3Co, 4W 15Cr, 16Mo, 5Fe	0.99	.323	14.7	94.8	2.38	2200	2515
Hastelloy B	3Co, 28Mo, 6Fe 4V, Bal Ni	1.01	.334	14.0	60.5	5.00	837	-----
Inconel X-750	73Ni, 7Fe, 15Cr, Bal miscel.	1.4	.298	16.7	84.0	5.00	1004	-----
Monel 400	66Ni, 1Fe, 33Cu	1.2	.319	13.8	72.0	5.00	933	-----
Nickel 200	99.5 Ni Bal misc.	1.1	.321	13.3	59.8	2.38	1780	2044
Ni-Be 440	98Ni, 2Be	2.7	.302	14.5	116.0	2.38	2580	2614
Stainless Steels 17-7PH	17Cr, 7Ni, Bal Fe	1.5	.276	10.1	91.0	5.00	1130	-----
446	25Cr, Bal Fe	0.83	.270	10.4	59.0	5.00	840	-----
304	9 Ni, 18Cr, Bal Fe	Full Hard 20-45	.290	17.3	200.0	2.41	3400	3586
Tantalum	99.9Ta	.33	.600	6.43	36.0	5.00	318	-----
Titanium	99.9 Ti	1.40	.160	9.53	28.0	5.00	828	-----
Tungsten	99.9W	-----	.70	4.50	132.0	5.00	853	-----
High Lead	-----	-----	-----	0-300°C	-----	-----	-----	-----
Glass Solder	-----	.1	-----	8.4	-----	-----	-----	-----
Forsterite	-----	-----	-----	68-932°F	-----	-----	-----	-----

## Appendix C

Gas and Surface Analysis Methods

This appendix gives a brief summary of the various analytical methods used to determine the gas and surface composition of the tested G-M tubes. Where possible, the reader is referred to technical or laboratory reports for detailed information.

Gas Analysis

Wet Chemical. The first and most quantitative method of bromine analysis was a wet chemical treatment. This work was performed by Mr. Brennen Gisclard of the Chemistry Branch of the Air Force Flight Dynamics Laboratory. He and his associates have developed a methyl orange reagent which is highly sensitive to halogen gases. Mr. Gisclard is presently involved in publishing a technical report containing the detailed information on this analytical method (Ref 9).

491 Mass Spectrometer. The second successful method of gas analysis was the use of a 491 Mass Spectrometer. This work was done by Mr. M. Taylor and supervised by Dr. M. Hughes. Both of these men are under the direction of Dr. Tiernan of the Chemistry Branch of the Air Force Aerospace Research Laboratory (ARL).

This method was not quantitative but did yield relative percentages of all gases contained within the G-M tube, (the results will be quantitative after known quantities of the gas are measured). This analysis was able to determine that bromine was not the only halogen gas within the counter, but that chlorine and iodine were also present in quantities of 1/20 that of bromine. It was not able to detect halogen gas in counters which exhibited oscillations and from the wet chemical analysis, this quantity is known to be  $<1.0 \mu\text{gm}$ .

Surface Analysis

Three different methods were used to investigate the structure and surface compositions of both the anode and cathode. These were: 21-110 spark source mass spectrometer, Auger spectrometry, and the scanning electron microprobe.

The Spark Source Spectrometer. The 21-110 spark source spectrometry was performed by the aforementioned individuals from the Chemistry Branch of ARL. This work gave the first confirmation of bromine reactions with the anode and cathode. This method is best explained in Ref 1:75. The results are not quantitative but do yield excellent relative measurements.

The Auger Spectrometer. Auger spectrometry was performed by Dr. T. W. Haas and Capt. George



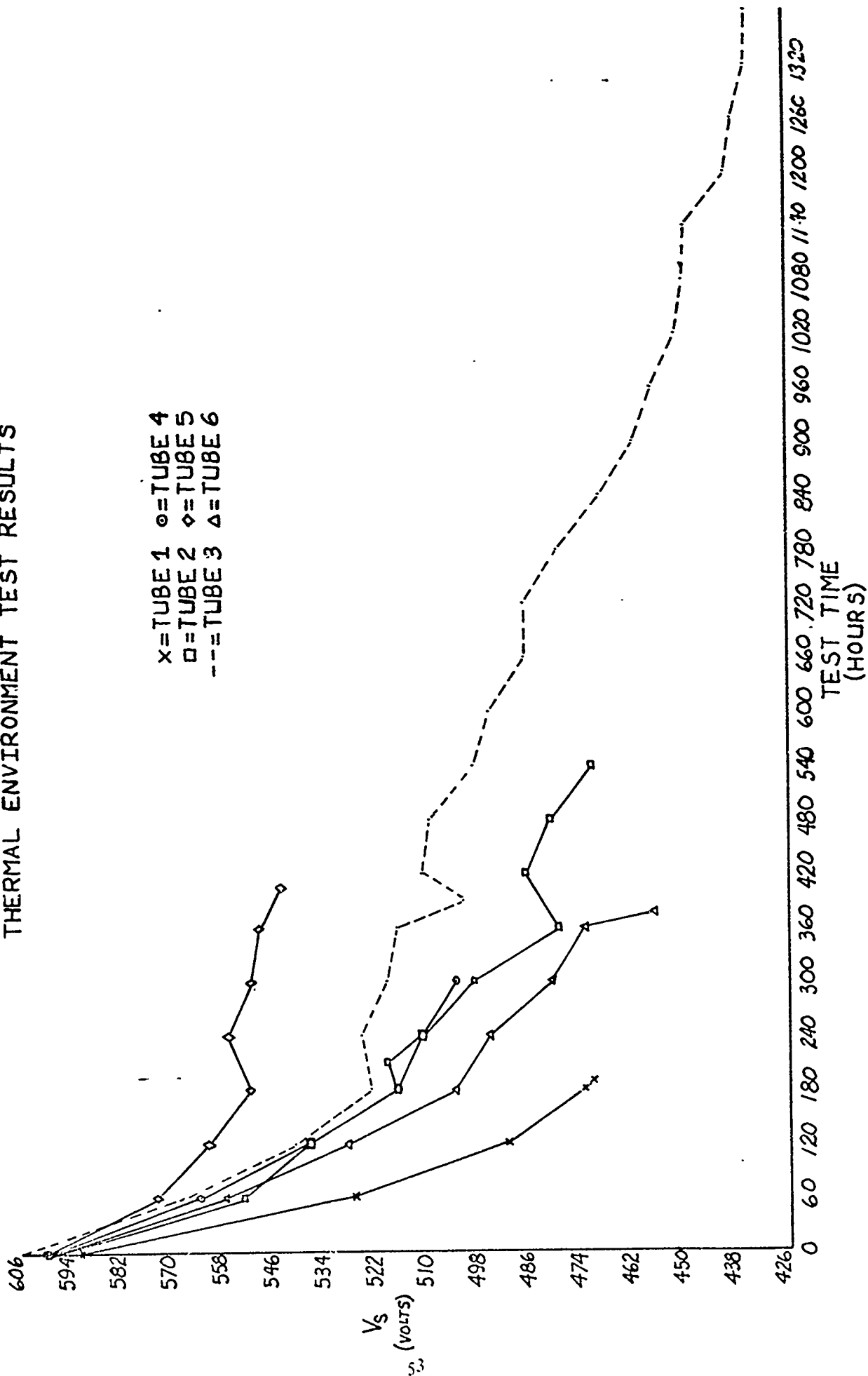
Dooley of the Surface Analysis Branch of the ARL. These results are also excellent comparative analyses but the greatest advantage is the determination of surface structure from 3 to 200Å in depth. This method is "almost" capable of giving quantitative results and excellent relative measurements can be gained. Detailed information into exact theory and procedures are contained in Ref 7:1-8.

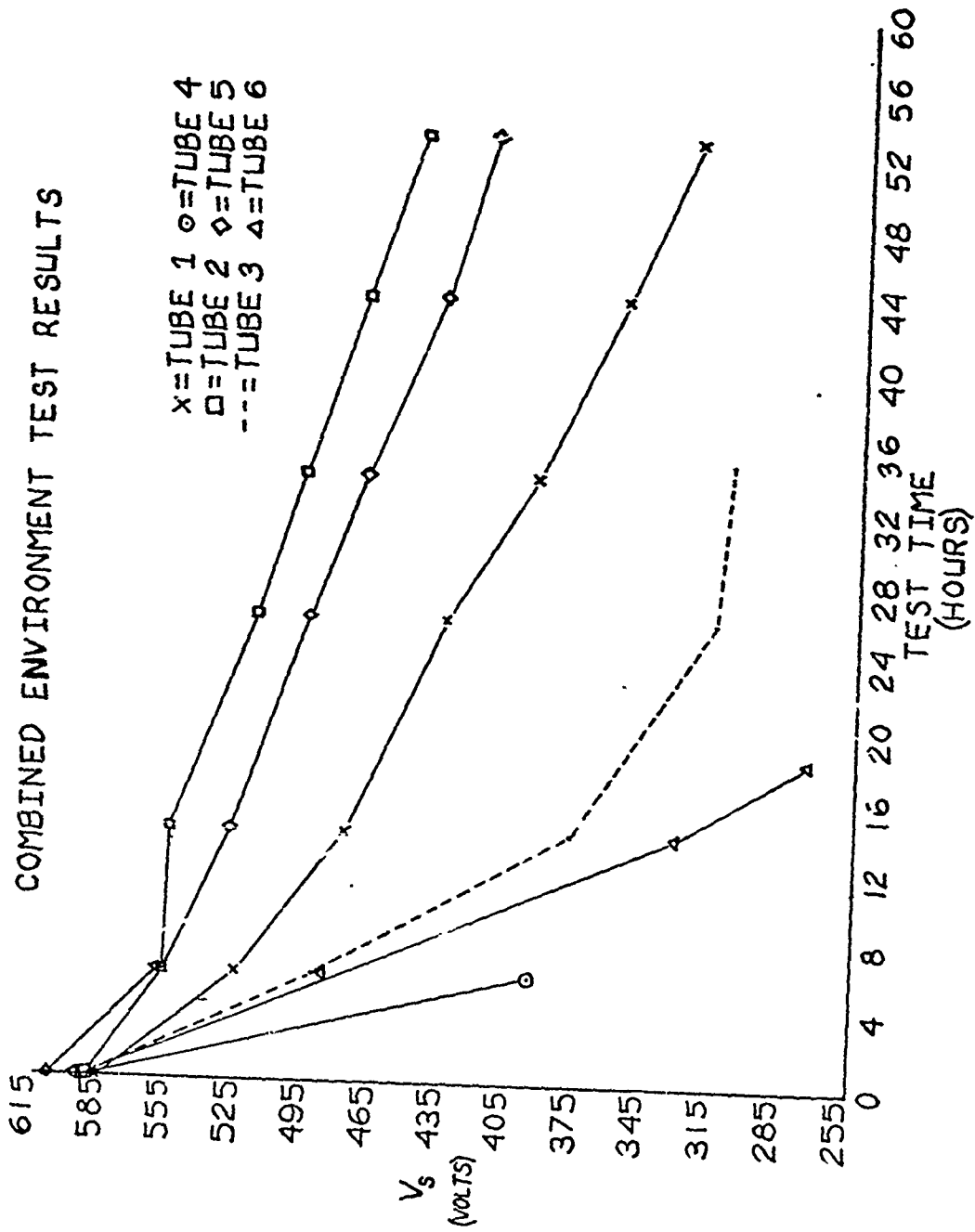
The Scanning Electron Microprobe. The scanning electron microprobe yields some excellent semi-quantitative and relative results. It is capable of determining layer thicknesses to 1.0 micron and providing polaroid pictures of all results. The advantages over the previous methods are: It has an extremely small beam (4 micron), it is able to continuously scan the sample surfaces, it can "backscatter line scan" for different species, and it yields photographs of all results. Some sample pictures and detailed information is contained in Ref 27:1-19. This analysis was performed by Mr. W. L. Baun and Mr. J. Solomon of the MAYA Branch of the USAF Materials Laboratory.

## Appendix D

### Graphic Data of the Changes in $V_s$ During the Environmental Tests

# THERMAL ENVIRONMENT TEST RESULTS





VITA

Dale Emory Morin [REDACTED]

[REDACTED] in 1958 and attended the University of Portland from which he received a Bachelor of Science degree and a commission in the USAF in 1962. After attending Undergraduate Pilot Training, he received his wings in December 1963. He served as a pilot in the 310th Air Refueling Squadron at Schilling Air Force Base, Kansas; Walker Air Force Base, New Mexico, and Plattsburgh Air Force Base, New York from January 1964 to August 1968. He served as a Forward Air Controller in Southeast Asia from April to December 1969. He attended Squadron Officers School at Maxwell Air Force Base, Alabama from January to April 1970.

[REDACTED]

This thesis was typed by Mrs. Sally Clemans